been suggested, no direct evidence has been reported indicating that SDF-1α induces macropinocytosis.

In this report, we synthesized dodeca-arginine (R12) bearing the phenyltrifluoromethyldiazirine moiety as a photocrosslinker with the hope of identifying the receptors responsible for the cellular uptake of oligoarginines (Figure 1A). We found that CXCR4 is a receptor that stimulates cellular uptake of the R12 peptide. Binding of R12 to CXCR4 stimulates actin organization and macropinocytosis. The binding of R12 to CXCR4 also leads to CXCR4 internalization. We also found that stimulating CXCR4 with its natural ligands, SDF-1α or gp120, triggered macropinocytosis together with internalization of the receptor. These results thus shed light on the roles of CXCR4 as a receptor for stimulating cellular uptake of arginine-rich CPPs and the induction of macropinocytosis, which may have implications in cellular responses, accompanied by intracellular delivery using oligoarginines, and in HIV infection.

RESULTS

CXCR4 as a Potential Target of R12 on Plasma Membranes

Photocrosslinking is a powerful methodology to detect molecular interactions in cells (Tomohiro et al., 2005). A biotin-tagged R12 peptide bearing trifluoromethyldiazirinephenylalanine (biotin-TmdPhe-R12) was designed to identify cell-surface molecules that can be recognized by the R12 peptide (Figure 1B). The R12 peptide was selected as a typical arginine-rich CPP with superior internalization efficiency, compared with the R8 and Tat peptides (Kosuge et al., 2008). Aryl-3-phenyl-3-trifluoromethyldiazirine derivatives are effective photocrosslinking agents and are readily incorporated into peptide chains using trifluoromethyldiazirinephenylalanine derivatives developed by Hatanaka and coworkers (Nakashima et al., 2006). The biotin tag was incorporated at the N terminus of the peptide together with a flexible linker (γ-aminobutyric acid) to facilitate the isolation of crosslinked proteins with the TmdPhe-R12 peptide. The biotin-TmdPhe-R12 peptide was thus prepared by Fmoc solid-phase peptide synthesis without difficulty.

HeLa cells pretreated with 0.5 μM biotin-TmdPhe-R12 at 37°C for 30 s were irradiated with UV light (365 nm) at 4°C for 3 min and washed with PBS prior to cell lysis. The peptide concentration and incubation time were set so that the peptide interacted with cell-surface molecules, but no significant endocytosed peptide signal was observed after examining the time course and the FITC-TmdPhe-R12 internalization methods (see Figure S1A available online). The biotin-TmdPhe-R4 peptide was used as a negative control; the R4 peptide showed no significant internalization (Futaki et al., 2001; Kosuge et al., 2008). After dialysis at 4°C for 12 hr, the samples were treated with streptavidin magnetic spheres for 1 hr. Proteins crosslinked with the R12 peptide were collected and the samples were subjected to SDS-PAGE (Figure 1C). Proteins corresponding to four major bands >240 kDa were specifically observed from cells treated with biotin-TmdPhe-R12 (arrows in Figure 1C) compared with those treated with biotin-TmdPhe-R4, and were digested with trypsin. The digested peptides were analyzed by MALDI-TOF mass spectrometry (MS) with peptide mass fingerprinting (PMF), and it was determined that the four bands were derived from myosin-9 (nonmuscle myosin heavy chain IIA). Involvement of myosin-9 in the endocytosis of CXCR4 and their colocalization on the cell surface, together with cell-surface exposure of myosin-9, has been suggested previously (Rey et al., 2007; Arii et al., 2010). Additionally, CXCR4 is expressed on the cell surface in a complex with syndecan-4 (Hamon et al., 2004). A western blot analysis of the proteins obtained using magnetic spheres from biotin-TmdPhe-R12-treated cells yielded positive staining with an anti-CXCR4 antibody, whereas no significant staining was observed for samples from biotin-TmdPhe-R4-treated cells (Figure 1D). Similarly, positive staining with anti-syndecan-4 antibody was observed for samples obtained from biotin-TmdPhe-R12-treated cells, which was almost twice as strong as that from biotin-TmdPhe-R4-treated cells (Figure 1D). These results suggest the possibility that CXCR4 plays a role in the cell-surface recognition of biotin-TmdPhe-R12.

CXCR4 as a Receptor to Promote R12 Uptake

The involvement of CXCR4 in the cellular uptake of R12 was then confirmed using CXCR4-knockdown HeLa cells, expressing 48% decreased levels of the receptor (Figure S1B). A significant decrease in R12-Alexa fluorescence signals was observed in the CXCR4-knockdown cells (Figure 1E, right) versus that in non-treated cells (Figure 1E, left) or in cells treated with negative-control siRNA (Figure 1E, middle). Fluorescence-activated cell sorting analysis showed a considerable decrease (32%) in the cellular uptake of the R12 peptide by CXCR4 knockdown under the same conditions (Figure 1F). Treating HeLa cells with the CXCR4-specific antagonist FC131 (cyclo[-D-Tyr-Arg-Arg-Nal-Gly-]) (Fujii et al., 2003) (10 μM) also resulted in a decrease in R12 peptide cellular uptake (Figure 1G). These results suggest the involvement of CXCR4 in the cellular uptake of R12.

(E and F) Downregulation of CXCR4 led to diminished cellular uptake of R12-Alexa, analyzed by confocal laser scanning microscopy without fixation (E) and by flow cytometry (F). Scale bars represent 50 μm. Peptide concentration, 10 μM. Data are shown as the mean ± SD of three independent experiments performed on different days. Asterisks indicate statistically significant differences compared to the negative-control cells. ****$p < 0.0001$ (unpaired Student's t test).

(G) Treating the cells with a CXCR4-specific antagonist, FC131, also inhibited the cellular uptake of R12-Alexa. Peptide and transferrin concentrations were 10 μM and 20 μg/ml, respectively. Data are shown as the mean ± SD of three independent experiments performed on different days. Asterisks indicate statistically significant differences compared to the negative-control cells. ****$p < 0.0001$ (two-way ANOVA followed by Bonferroni's post hoc test).

(H) Live cell analysis of the colocalization of R12-Alexa568 with CXCR4-Venus on the cell surface. Cells were treated with 5 μM R12-Alexa568 for 10 min at 4°C and the surfaces of live cells facing the bottom glass were observed by confocal laser scanning microscopy. Scale bars represent 5 μm.

(I) Treatment with the Gi signaling-pathway inhibitor PTX (100 ng/ml) yielded decreased cellular uptake of R12-Alexa but not R8- or Tat-Alexa. Peptide and transferrin concentrations were 10 μM and 50 μg/ml, respectively. Data are shown as the mean ± SD of three or four values obtained from independent experiments performed on different days. Asterisks indicate statistically significant differences from the no-inhibitor groups. ****$p < 0.0001$ (two-way ANOVA followed by Bonferroni's post hoc test).

See also Figure S1.

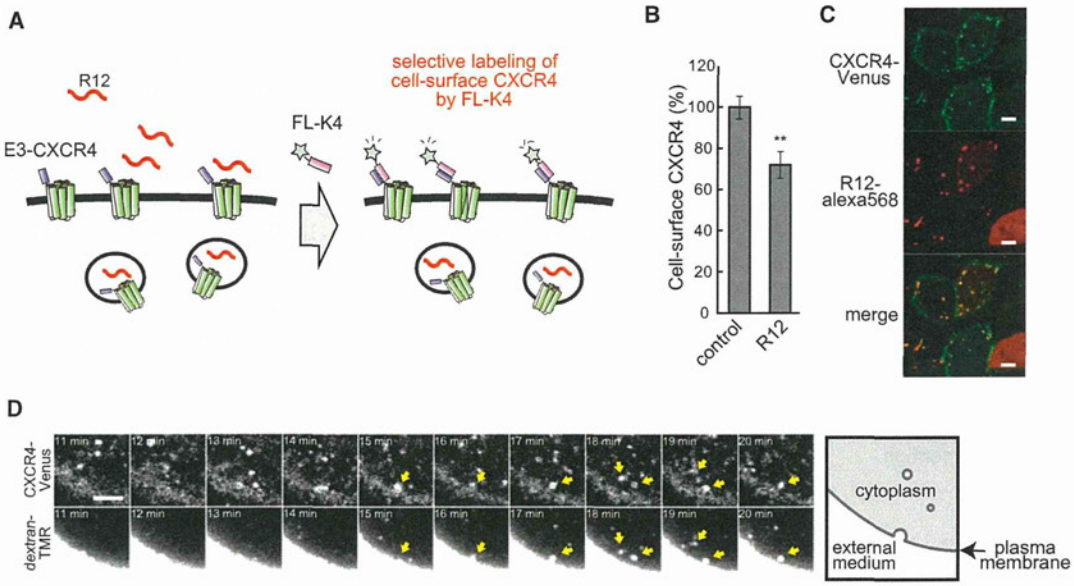

Figure 2. Internalization of CXCR4 by Treatment with R12

(A) Specific labeling of E3-tagged CXCR4 on cell surfaces using fluorescently labeled K4 probe.

(B) Internalization of CXCR4 following R12 treatment. CHO cells expressing E3-CXCR4 were treated with nonlabeled R12 (10 μM) for 30 min, and then the amount of the CXCR4 remaining on the cell surface was analyzed by treatment with E3-specific fluorescein-labeled K4 peptide (FL-K4). Data are shown as the mean ± SD of three independent experiments. Asterisks indicate statistically significant differences from control cells. $^{**}p < 0.01$ (unpaired Student's t test).

(C) Colocalization of R12 with CXCR4 after cell treatment with 5 μM R12-Alexa568 for 30 min at 37°C. The live cells were then analyzed directly by confocal laser scanning microscopy without fixation. Scale bars represent 5 μm.

(D) CXCR4 internalizes into cells with the macropinocytosis marker dextran-TMR (70 kDa). CHO-C4V cells were treated with 10 μM nonlabeled R12 together with dextran-TMR (1 mg/ml) and observed by time-lapse imaging. Significant colocalization of the CXCR4-Venus and dextran-TMR signals was observed, suggesting that they were captured in the same endosomal vesicles. Yellow arrows indicate that the vesicles contain both CXCR4-Venus and dextran-TMR. The scale bar represents 5 μm.

See also Figure S2.

Interestingly, no significant reduction in R8 or Tat (10 μM) cellular uptake was observed in CXCR4-knockdown cells (Figure 1F), and similar patterns were observed in FC131-treated cells (Figure 1G). Thus, CXCR4 was not responsible for the cellular uptake of these peptides. The R8 and Tat peptides are typical arginine-rich CPPs with a smaller number of arginines in their sequences than R12 (Futaki, 2006; Kosuge et al., 2008), suggesting diversity in cellular uptake mechanisms even among arginine-rich peptides.

Cell-surface interaction of CXCR4 with R12 was confirmed by confocal laser scanning microscopy (Figure 1H). We established CHO cells stably expressing CXCR4 (CHO-C4V) in which a fluorescent protein, Venus, was tagged to the CXCR4 C terminus (cytoplasmic side). Cells were treated with Alexa 568-labeled R12 peptide (R12-Alexa568) at 4°C for 10 min, conditions under which endocytosis does not occur. Significant colocalization of the CXCR4 signals with R12 (Figure 1H) suggested specific binding of R12 to CXCR4 on the cell surface, whereas lower levels of colocalized signals were observed when the cells were treated with Alexa 568-labeled R8 and Tat peptides (Figure S1C).

Binding of CXCR4 to its natural ligand, SDF-1α, leads to actin reorganization via the Gi protein-signaling pathway (Möhle et al., 2001). Indeed, a marked lamellipodia (i.e., thin, veil-like extensions at the edge of cells that contain a dynamic array of actin filaments, typically observed for cells treated with oligoarginine CPPs) formation was observed for control cells by treatment with R12 for 20 min; however, no significant alteration in actin structure was observed in CXCR4-knockdown cells (Figure S1D). Cellular uptake of R12-Alexa was suppressed by 30% in the presence of pertussis toxin (PTX), an inhibitor of the Gi protein-signaling pathway (Phillips and Ager, 2002) (Figure 1I). Furthermore, PTX treatment also led to a significant suppression in the formation of lamellipodia by the R12 peptide (data not shown). These results suggest that CXCR4 serves as an R12 receptor to promote actin organization, together with uptake of the R12 peptide. Involvement of the Gi protein-signaling pathway was suggested in the above process. Here again, cellular uptake of R8 and the Tat peptide was not affected by PTX treatment (Figure 1I).

Treating cells with the R12 peptide led to internalization of the CXCR4 receptor. A coiled-coil tag/probe system, developed by Yano et al. (2008), was used to analyze this result. Specifically, CXCR4 bearing a surface-exposed tag sequence E3 $(EIAALEK)_3$ at the N terminus (E3-CXCR4) was expressed on CHO-K1 cells (Figure 2A). After treating the cells with R12 or other CXCR4 ligands, E3-CXCR4 remaining on the plasma membranes was quantified by a fluorescently labeled E3-specific peptide probe, K4 $(KIAALKE)_4$. This system was expected to more accurately assess the quantities of cell surface-exposed receptors,

compared with conventional methods that use receptor-specific antibodies; binding of receptor-specific antibodies may be hampered when their ligands are tightly bound to the receptor. However, the relatively small K4 probe used in this system allowed us to detect CXCR4 without disruption by ligand binding (Yano et al., 2008). Treating the cells with R12 peptide for 30 min resulted in the internalization of cell-surface CXCR4; an ~30% decrease in the amount of CXCR4 on cell surfaces was observed following this treatment compared with nontreated cells (Figure 2B).

The intracellular fate of CXCR4 after binding with R12 was then analyzed using the CXCR4-Venus system employed in Figure 1H, but this time cells were incubated at 37°C to allow endocytic cellular uptake. Treatment of the cells with R12-Alexa for 30 min led to internalization of CXCR4 and significant colocalization of the R12-Alexa568 signal with CXCR4 in the cytoplasm (Figure 2C). On the other hand, large amounts of CXCR4 remained on the cell surface, even after treatment with R8- and Tat-Alexa568, which yielded considerably fewer colocalized signals in the cytoplasm compared to R12 treatment (Figure S2A). Time-lapse imaging of CXCR4-Venus cells treated with a macropinosome marker (70 kDa dextran labeled with tetramethylrhodamine; dextran-TMR) in the presence of R12 peptide showed significant colocalization of the signals of Venus and TMR, indicative of CXCR4 internalization via the macropinocytic pathways stimulated by the R12 peptide (Figure 2D). Because endosomes formed by macropinocytosis (i.e., macropinosomes) can be CXCR4-Venus signals colocalizing with dextran-TMR, compared with those without significant colocalization (see Figure S2B), this also suggests that these signals represent macropinosomes. Thus, CXCR4 serves as a receptor of R12 and is internalized into cells via macropinocytosis together with R12.

Note that the above observation would not necessarily indicate CXCR4-mediated macropinocytosis as the sole and exclusive pathway for R12 uptake. R8 and other arginine-rich peptides also employ macropinocytosis for their cellular uptake (Nakase et al., 2004); as shown in this study, the methods are not identical to that using CXCR4. However, it could be possible that a part of R12 may also be internalized in the cells using similar methods employed by R8. Dynasore is an inhibitor of dynamin that is critically involved in clathrin- or caveolae-mediated endocytosis. Treating the cells with dynasore yielded an ~35% decrease in 5 μM R12 uptake (Figure S2C). This result suggests the possibility that certain dynamin-dependent endocytic pathways may be involved in the cellular uptake of R12 simultaneously with macropinocytosis. Additionally, only an ~10% reduction in the cellular uptake of R8 was observed under the same dynasore treatment (Figure S2C). The relative insensitivity of R8 uptake by dynasore may again suggest differences in the methods of cellular uptake between R12 and R8.

Stimulation of CXCR4 by SDF-1α or HIV-1 gp120 Also Leads to Macropinocytosis

If stimulating CXCR4 with R12 induces actin organization and its macropinocytic uptake, it is possible that stimulating the receptor with other ligands may also stimulate macropinocytosis. SDF-1α is a typical CXCR4 ligand, and the involvement of actin reorganization through CXCR4 activation has been reported (Voermans et al., 2001; Wu and Yoder, 2009). It has been reported that ligand binding to CXCR4 leads to its internalization via clathrin-dependent endocytosis (Signoret et al., 1997; Orsini et al., 1999; Venkatesan et al., 2003). However, there is no report of the relevance of actin reorganization through CXCR4 activation to macropinocytosis induction. In this context, we examined whether stimulation of CXCR4 with SDF-1α may lead to macropinocytosis in addition to actin organization and an eventual increase in its cellular uptake.

Treating HeLa cells with SDF-1α led to an increase in cellular uptake of 70 kDa dextran of ~110%, and the increase in 70 kDa dextran uptake by SDF-1α stimulation was inhibited by 40% in the presence of ethylisopropylamiloride (EIPA), a typical macropinocytosis inhibitor (Nakase et al., 2004) (Figure 3A). SDF-1α also induces actin organization, and significant lamellipodia formation was also observed for SDF-1α-treated cells (Figure 3B). These observations suggest the induction of macropinocytosis following CXCR4 stimulation with its natural ligand SDF-1α. Quantifying the cell-surface receptor using E3-tagged CXCR4, as used in Figure 2B, showed that stimulating CXCR4 with SDF-1α led to a decrease in cell surface-expressed CXCR4 by ~65% (Figure 3C). A confocal microscopic analysis showed that CXCR4 tagged with Venus was internalized into the cells following treatment with SDF-1α (Figure 3D). Colocalization of the CXCR4-Venus signals with those of 70 kDa dextran suggests the localization of CXCR4 in macropinosomes. To the best of our knowledge, this is the first demonstration that stimulating CXCR4 with SDF-1α leads to macropinocytosis and the eventual internalization of CXCR4.

Considerable research has focused on macropinocytosis and its relevance to viral infections (Mercer and Helenius, 2009). We not only identified CXCR4 as a receptor that induces macropinocytosis but also showed that the receptor is internalized in cells and is trapped in macropinosomes bound to its ligand. HIV infection of target cells is accomplished on the cell surface, and CXCR4 serves as a CD4 protein coreceptor to stimulate viral binding and successive fusion to the plasma membranes, allowing entry of the viral nucleocapsid. Thus, if HIV binding to CXCR4 induces macropinocytosis, HIV may become trapped in macropinosomes and delivered to cells.

HIV-1 gp120 is a glycoprotein present on the surface of the viral envelope and is essential for CXCR4 binding, leading to virus entry into cells (Tamamura et al., 2005). Treatment of HeLa cells with 500 nM gp120 induced a 25% increase in 70 kDa dextran uptake in 60 min (Figure 3E). Significant lamellipodia formation was also observed 20 min after administering gp120 (Figure 3B). These results suggest that macropinocytosis may accompany HIV entry into cells (Wu and Yoder, 2009).

Effect of R12 Treatment and Macropinocytosis on HIV Infection of Host Cells

HIV-1_{IIIB} is a subtype of HIV-1 that uses CXCR4 as a coreceptor for entry into susceptible cells. Anti-HIV infection activity of R12 for HIV-1_{IIIB} was analyzed using a T cell line, MT-4, which is highly susceptible to HIV infection (Koyanagi et al., 1985). The cells were incubated with HIV-1_{IIIB} in the presence of R12 or R8 for 5 days and cell viability was analyzed using the MTT (3-[4,5-dimethylthiazol-2-yl]-2,5-diphenyltetrazolium bromide) assay as reported previously (Kodama et al., 2001), yielding a 50%

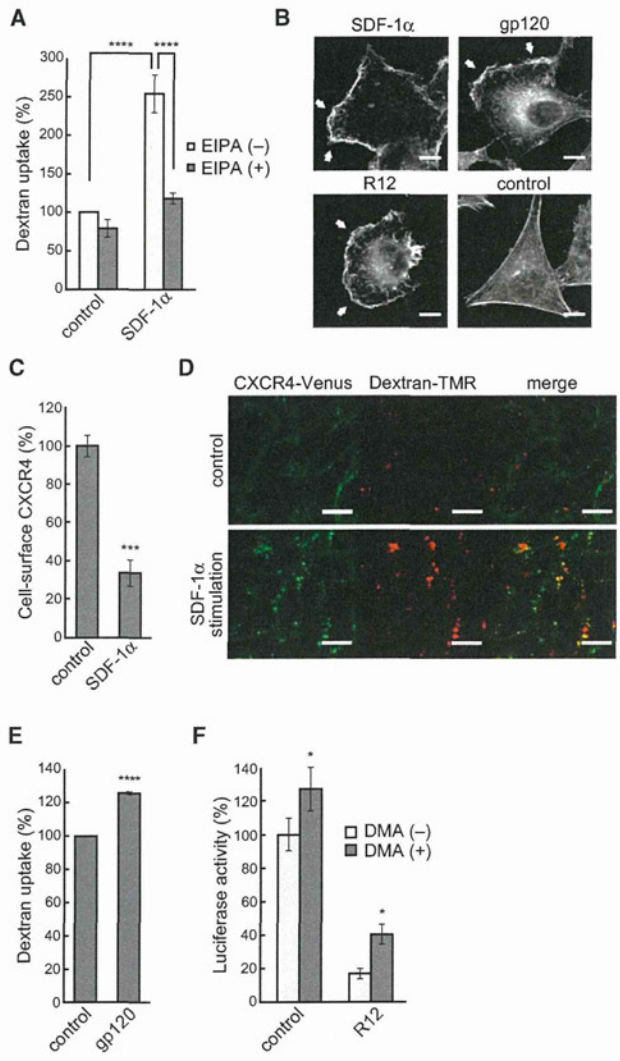

Figure 3. Stimulating CXCR4 with SDF-1α and gp120 Induces Actin Organization and Macropinocytosis

(A) Increase in 70 kDa dextran-fluorescein uptake in HeLa cells following treatment with 100 nM SDF-1α for 1 hr. Pretreatment with EIPA (100 μM) diminished the dextran uptake. Data are shown as the mean ± SD of three independent experiments. Asterisks indicate statistically significant differences from control cells. ****$p < 0.0001$ (two-way ANOVA followed by Bonferroni's post hoc test).

(B) Actin cytoskeleton rearrangement by SDF-1α and gp120. HeLa cells were treated with SDF-1α (100 nM), gp120 (500 nM), and R12 (10 μM) for 20 min. The cells were fixed with 4% paraformaldehyde, and cellular F-actin was stained with phalloidin-tetramethylrhodamine isothiocyanate. White arrows indicate lamellipodia. Scale bars represent 10 μm.

(C) Internalization of CXCR4 following treatment with 100 nM SDF-1α (30 min). The experiments were conducted using E3-CXCR4 cells and FL-K4 as in Figure 2B. Data are shown as the mean ± SD of three independent experiments. Asterisks indicate statistically significant differences from control cells. ***$p < 0.001$ (unpaired Student's t test).

(D) Treating CHO-C4V cells with 100 nM SDF-1α led to the internalization of CXCR4-Venus by cells. CXCR4-Venus signals showed high colocalization with the macropinosome marker 70 kDa dextran-TMR. Control cells showed less internalization of CXCR4-Venus and 70 kDa dextran-TMR, yielding little colocalization with 70 kDa dextran-TMR signals. Scale bars represent 10 μm.

(E) HIV-1 envelope protein gp120 (500 nM) induces macropinocytosis. HeLa cells were treated with 500 nM gp120, as shown in (A), for 1 hr. Data are shown as the mean ± SD of three independent experiments. Asterisks indicate statistically significant differences from control cells. ****$p < 0.0001$ (unpaired Student's t test).

(F) Inhibition of HIV infection in the presence of a macropinocytosis inhibitor. MT-4 cells were pretreated with DMA for 30 min at 37°C. HIV-based luciferase expression vector pseudotyped with HIV-1_{IIIB} envelope was used to infect DMA-treated or untreated cells in the absence or presence of 5 μM R12. After 48 hr of culture, luciferase activity was measured. Data are shown as the mean ± SD of three independent experiments performed in duplicate. Asterisks indicate statistically significant differences from cells treated without inhibitor. *$p < 0.05$ (unpaired Student's t test).

Table 1. Antiviral Activities against HIV-1_{IIIB} Determined by MTT Assay

Peptide	Mean EC_{50} (nM) ± SD	Mean CC_{50} (nM) ± SD
R12	394 ± 28	>1,000
R8	>1,000	>1,000

Data shown are means and standard deviations obtained from three independent assays.

effective concentration (EC_{50}) of 394 ± 28 nM for the R12 peptide and >1,000 nM for R8 (Table 1). The 50% cytotoxic concentration (CC_{50}) of both peptides was >1,000 nM. The anti-HIV activity of R12 for HIV-1_{IIIB} was also confirmed using a single-round MAGI assay (multinuclear activation of a galactosidase indicator assay; Kimpton and Emerman, 1992) with an EC_{50} value of 332 ± 76 nM (AZT reference, 22 ± 2 nM) (Table 2), whereas no inhibitory effect of R12 (EC_{50} > 10 μM; AZT reference, 23 ± 8 nM) was observed for HIV-1_{BaL} infection using CCR5, instead of CXCR4, as a coreceptor. This suggests that CXCR4 is the target for R12 inhibition or that the internalization of the receptor results in HIV entry inhibition.

Macropinocytosis stimulates internalization of CXCR4 as well as viral uptake into endosomes, which may decrease the chance of HIV entry into host cells via cell-surface fusion (Schaeffer et al., 2001). The effect of macropinocytosis on HIV entry was also assessed using an HIV-1-based firefly luciferase expression vector pseudotyped with HIV-1_{IIIB} envelope. MT-4 cells were treated with dimethylamiloride (DMA), a typical inhibitor of macropinocytosis that has been employed for the analysis of dendritic cell-mediated HIV-1 endocytosis (Maréchal et al., 2001), for 30 min prior to infection and incubated for 48 hr. Treatment of the cells with DMA resulted in an ~30% increase in luciferase activity, suggesting that inhibition of macropinocytosis improves viral infection (Figure 3F, left). There was a significant decrease (~70%) in luciferase activity in the presence of R12, confirming the HIV inhibitory effect of the peptide (Figure 3F, right). However, this effect was diminished by pretreatment with DMA (Figure 3F, right).

DISCUSSION

Scientific interest in arginine-rich CPPs has been increasing due to their ability to bring exogenous molecules into cells. The ability of arginine-rich CPPs to induce macropinocytosis is one explanation for their cellular uptake. Although several membrane proteins have previously been considered as potential

Table 2. Antiviral Activities Determined by MAGI Assay

	Mean EC_{50} (nM) ± SD	
Strain	R12	AZT
HIV-1_{IIIB}	332 ± 76	22 ± 2
HIV-1_{BaL}	>10,000	23 ± 8

Data shown are means and standard deviations obtained from three independent assays. AZT (a nucleoside analog reverse-transcriptase inhibitor) was used as a control.

candidates that activate macropinocytosis, or even other forms of endocytosis, specifically responsible for the cellular uptake of arginine-rich CPPs, no substantive receptor has been identified. It has been reported, for example, that the full-length Tat protein (86 residues) could activate a vascular endothelial growth factor receptor (Mitola et al., 1997), but the basic domain (positions 46–64 of the Tat protein corresponding to the CPP segment) was not a high-affinity ligand for the receptor (Rubio Demirovic et al., 2003). It has also been reported that the full-length Tat protein binds to CXCR4 and works as an antagonist against the infection of HIV (Xiao et al., 2000). Interestingly, the basic segment corresponding to the CPP segment (residues 48–60) was not responsible for the antagonism activity but rather residues 11–50 of the Tat protein containing the cysteine-rich domain. Therefore, it seems likely that the receptors for the full-length Tat protein may not necessarily work for the receptor of the arginine-rich CPPs. We and others have reported that the interaction of the arginine-rich peptides with the membrane-associated proteoglycans, including syndecans, quickly activates the Rac protein and induces actin organization and macropinocytosis (Gerbal-Chaloin et al., 2007; Nakase et al., 2007, 2009; Letoha et al., 2010). Although the interaction of arginine-rich peptides with membrane-associated proteoglycans may lead to their multimerization to induce actin polymerization, more evidence is required to conclude that these proteoglycans are actual receptors that can induce macropinocytosis; as is seen in the case of FGF2 (Ishihara, 1993), proteoglycans often couple with other receptors to activate them. Additionally, it was recently reported that a complex of oligonucleotides with the stearylated TP-10 analog PepFect14 was taken into cells through scavenger receptors (Ezzat et al., 2012). This was an important finding that may potentially be extendable to enhance the biological effects given by the oligonucleotides. However, recognition of the negative charges of the complex by the receptor, not of the peptides, is considered to be the mechanism.

Using synthetic peptides as chemical tools, we have demonstrated that the CXCR4 chemokine receptor acts as a receptor to stimulate cellular uptake of the R12 peptide. Cellular uptake of R12 was inhibited by CXCR4 siRNA knockdown and by FC131, an antagonist of CXCR4. Treating the cells with R12 led to actin organization (lamellipodia formation) and macropinocytosis, but CXCR4 knockdown effectively prevented the formation of lamellipodia. Confocal microscopy revealed significant colocalization of CXCR4 with the R12 peptide on cell surfaces. Binding of R12 to CXCR4 led to their internalization, and significant colocalization of these signals was observed in macropinosomes in the cells. Treatment of the cells with PTX suppressed the cellular uptake of R12, suggesting the use of a Gi signaling pathway for uptake.

To our knowledge, these results are not only the first report of a substantive receptor to stimulate the uptake of arginine-rich CPPs, but are also the first illustration of intracellular traffic of the receptors involved in R12 uptake after ligand activation. Interestingly, R8 and Tat, other typical arginine-rich CPPs, did not significantly activate this CXCR4-mediated uptake pathway. These peptides are also reported to use macropinocytosis for their cellular uptake (Nakase et al., 2004, 2007). R12 has a higher internalization efficiency than the R8 and Tat peptides (Nakase et al., 2007; Kosuge et al., 2008), and the higher valency of the guanidino groups in a peptide to ensure greater interaction with cell-surface molecules has been suggested as one explanation (Futaki, 2006; Wender et al., 2008). However, the present study indicates that the lack of CXCR4-mediated activation of macropinocytosis by R8 and Tat may explain the higher cellular uptake efficiency of R12 over these peptides. In addition, if the cooperation of CXCR4 and syndecan-4 is important for receptor activation, R12 may stabilize these complex structures.

We also found that stimulation of CXCR4 with an intrinsic ligand, SDF-1α, induced macropinocytosis. This study also suggests that macropinocytosis is induced by the interaction of HIV-1 with CXCR4 on host cell membranes, which leads to the internalization of the receptor during viral infection of the host cells. Although the involvement of macropinocytosis with HIV-1 internalization has been observed in specific cells such as dendritic cells (Wang et al., 2008), macropinocytosis operates only for housekeeping in these cells, and there should be distinct differences in the methods of internalization in the many cells where macropinocytosis is induced only by external stimuli. Our study suggests that macropinocytosis stimulates internalization of CXCR4 as well as viral uptake into late endosomes, which may decrease the chance of HIV entry into host cells via cell-surface fusion and promote viral degradation in endosomes (Schaeffer et al., 2001). Thus, macropinocytosis induced by the interaction with HIV-1 may eventually work as a protective response by host cells against a viral invasion. In this context, R12 shows inhibitory activity against HIV-1 infection; interaction of R12 with CXCR4 leads to internalization of the receptor as well as viral uptake via macropinocytosis, both of which may inhibit viral infection. ALX40-4C is an anti-HIV-1 peptide (acetyl-[D-Arg]$_9$-amide) (Doranz et al., 1997; Zhang et al., 2002), having structural similarity with R8 and R12. The anti-HIV-1 activity of ALX40-4C has been claimed to be exclusively by blocking virus-CXCR4 interactions (Doranz et al., 2001), and this would also be one mechanism of the anti-HIV-1 activity of R12. Detailed studies of the effect of ALX40-4C on CXCR4 internalization and macropinocytosis induction would be beneficial to better understand the contribution of macropinocytosis to the inhibition of HIV-1 infection.

SIGNIFICANCE

This report has shed light on the roles of CXCR4 as a receptor for stimulating cellular uptake of arginine-rich cell-penetrating peptides and the induction of macropinocytosis, which should have implications for cellular responses, accompanied by intracellular delivery using oligoarginines, and for HIV infection.

EXPERIMENTAL PROCEDURES

Preparation of Biotin-TmdPhe-R12 and Biotin-TmdPhe-R4

H-GABA-TmdPhe-Gly-(Arg[Pbf])$_{12}$-NH-resin (GABA, γ-aminobutyric acid; Pbf, 2,2,4,6,7-pentamethyldihydrobenzofuran-5-sulfonyl) was prepared by Fmoc (9-fluorenylmethyloxycarbonyl) solid-phase peptide synthesis on a Rink amide resin, as described previously (Kosuge et al., 2008; Nakase et al., 2009), in which the TmdPhe was assembled into the peptide chain using Fmoc-TmdPhe, as is the case with other amino acids. Biotin was then introduced onto the peptide resin using biotinamidohexanoic acid N-hydroxysuccinimide ester (Sigma) to yield biotinamidohexanoyl-GABA-TmdPhe-Gly-(Arg[Pbf])$_{12}$-NH-resin. The peptide was deprotected and cleaved from the resin by treatment with a trifluoroacetic acid/ethanedithiol mixture (95:5), followed by reverse-phase high-performance liquid chromatography purification to yield biotinamidohexanoyl-GABA-TmdPhe-Gly-(Arg)$_{12}$-amide (biotin-TmdPhe-R12). The mass of the product was confirmed by MALDI-TOF MS: 2629.99 (calculated for $[M+H]^+$ 2629.14). Biotin-TmdPhe-R4 was similarly prepared as biotin-TmdPhe-R12. MALDI-TOF MS: 1380.81 (calculated for $[M+H]^+$ 1379.61).

Photocrosslinking

HeLa cells (1.2×10^6) were plated on 100 mm dishes and cultured in α-minimum essential medium (α-MEM) containing 10% heat-inactivated bovine serum (α-MEM/BS) for 48 hr. After the cells were washed three times with PBS(+), they were treated with biotin-TmdPhe-R12 (0.5 μM) or biotin-TmdPhe-R4 (1.5 μM) for 30 s at 37°C and then irradiated with a UV lamp with a 365 nm filter for 3 min at 4°C. Cells were washed with PBS(+) twice and lysed in RIPA buffer (100 μl) containing 150 mM NaCl, 10 mM Tris-HCl (pH 7.2), 0.1% SDS, 1.0% NP-40, 1% deoxycholate, and 5 mM EDTA. Lysates were then dialyzed against 1,000 ml PBS at 4°C for 12 hr using a Slide-A-Lyzer (molecular weight cutoff 20,000; Pierce).

The protein concentration of the above lysates was adjusted to yield 500 μg protein/500 μl RIPA buffer, and 10% SDS (214 μl) in water was added to yield a protein solution containing 3% SDS. Streptavidin magnetic spheres (Promega; 300 μl) were then added to the solution. After gently mixing at 20°C for 1 hr, the streptavidin magnetic spheres, bearing proteins crosslinked with biotin-TmdPhe-R12, were collected with a magnet and washed with RIPA buffer, and then the sample buffer for SDS-PAGE (40 μl) containing 3% SDS and 10% 2-mercaptoethanol was added. After heat denaturation at 85°C for 5 min, the mixtures were subjected to electrophoresis. Prior to PMF analysis, the samples were analyzed by 7.5% SDS-PAGE using silver staining. Protein bands positive in biotin-TmdPhe-R12-treated cells but negative in biotin-TmdPhe-R4-treated cells were collected, trypsinized, and subjected to MALDI-TOF MS/PMF analysis. Western blotting was conducted using 10% SDS-PAGE prior to sample transfer to PVDF membranes. Anti-CXCR4 antibody (1:1,000; ab2074; Abcam), anti-syndecan-4 antibody (1:1,000 dilution; 5G9; Santa Cruz Biotechnology), and anti-CD71 antibody (1:200 dilution; sc-9099; Santa Cruz Biotechnology), together with the corresponding second antibody conjugated to horseradish peroxidase, were used to detect the target proteins.

Confocal Microscopic Observation of CXCR4-Venus and R12-Alexa

CHO-C4V cells (4×10^5 cells/well) stably expressing CXCR4-Venus (see Supplemental Experimental Procedures) were plated on 35 mm glass-bottomed dishes and cultured in an F-12 nutrient mixture containing 10% heat-inactivated fetal bovine serum (F-12/FBS) supplemented with penicillin/streptomycin and hygromycin for 72 hr. After complete adhesion, the cell-culture medium was changed to serum-free F-12 and cells were incubated for 1 hr. The cells were then incubated at 37°C in fresh medium (150 μl) containing 5 μM R12-Alexa568. The cells were washed twice with heparin/PBS, and ice-cold fresh medium without peptides (1 ml) was added. Localization of R12-Alexa568 and CXCR4-Venus in the cells was then analyzed using an FV1000 confocal scanning laser microscope (Olympus) equipped with a 60× objective without fixing the cells. Colocalization with dextran-TMR (70 kDa) was analyzed by incubating CHO-C4V cells with fresh medium containing 10 μM R12 or 100 nM SDF-1α in the presence of 1 mg/ml dextran-TMR for 20 min at 37°C.

To observe CXCR4-Venus and R12-Alexa568 on the cell surface, cells were incubated with serum-free F-12 for 30 min at 4°C and treated with 5 μM R12-Alexa568 for 10 min at 4°C to prevent internalization of CXCR4-Venus. The cells were washed with ice-cold F-12 twice and analyzed with a confocal scanning laser microscope as described above.

Colocalization of R8-Alexa568 and Tat-Alexa568 with CXCR4 was also observed using confocal microscopy similar to that with R12-Alexa568.

CXCR4 Internalization Assay

E3-CXCR4 CHO cells were similarly established as the CHO-C4V cells, and were detached using Versene. Cells (0.4×10^6) were resuspended in F-12 medium containing R12 or SDF-1α (500 μl), incubated at 4°C or 37°C for 30 min, and washed twice with ice-cold PBS containing 0.5% (w/v) heparin and PBS. The cells were treated with 100 nM fluorescein-labeled K4 peptide (FL-K4) (Yano et al., 2008) in F-12 (100 μl) at 4°C for 15 min and analyzed using a FACSCalibur flow cytometer. Ten thousand events were analyzed per sample (n = 3).

SUPPLEMENTAL INFORMATION

Supplemental Information includes three figures and Supplemental Experimental Procedures and can be found with this article online at http://dx.doi.org/10.1016/j.chembiol.2012.09.011.

ACKNOWLEDGMENTS

This work was supported in part by Grants-in-Aid for Scientific Research and the Targeted Protein Research Program from the Ministry of Education, Culture, Sports, Science and Technology of Japan. R.M. is grateful for research fellowships from the Japan Society for the Promotion of Science for Young Scientists. This study was also supported by the Swedish Research Council, the Swedish Foundation for Strategic Research, and the Swedish Governmental Agency for Innovation Systems (project no. MDB09-0015) (to Ü.L. and A.G.), and the Strategic Japanese-Swedish Cooperative Program on "Multidisciplinary BIO" from the Japan Science and Technology Agency and VINNOVA (to S.F.).

Received: July 23, 2012
Revised: August 28, 2012
Accepted: September 3, 2012
Published: November 21, 2012

REFERENCES

Arii, J., Goto, H., Suenaga, T., Oyama, M., Kozuka-Hata, H., Imai, T., Minowa, A., Akashi, H., Arase, H., Kawaoka, Y., and Kawaguchi, Y. (2010). Non-muscle myosin IIA is a functional entry receptor for herpes simplex virus-1. Nature *467*, 859–862.

Conner, S.D., and Schmid, S.L. (2003). Regulated portals of entry into the cell. Nature *422*, 37–44.

Doranz, B.J., Grovit-Ferbas, K., Sharron, M.P., Mao, S.-H., Goetz, M.B., Daar, E.S., Doms, R.W., and O'Brien, W.A. (1997). A small-molecule inhibitor directed against the chemokine receptor CXCR4 prevents its use as an HIV-1 coreceptor. J. Exp. Med. *186*, 1395–1400.

Doranz, B.J., Filion, L.G., Diaz-Mitoma, F., Sitar, D.S., Sahai, J., Baribaud, F., Orsini, M.J., Benovic, J.L., Cameron, W., and Doms, R.W. (2001). Safe use of the CXCR4 inhibitor ALX40-4C in humans. AIDS Res. Hum. Retroviruses *17*, 475–486.

Ezzat, K., Helmfors, H., Tudoran, O., Juks, C., Lindberg, S., Padari, K., El-Andaloussi, S., Pooga, M., and Langel, U. (2012). Scavenger receptor-mediated uptake of cell-penetrating peptide nanocomplexes with oligonucleotides. FASEB J. *26*, 1172–1180.

Falcone, S., Cocucci, E., Podini, P., Kirchhausen, T., Clementi, E., and Meldolesi, J. (2006). Macropinocytosis: regulated coordination of endocytic and exocytic membrane traffic events. J. Cell Sci. *119*, 4758–4769.

Fujii, N., Oishi, S., Hiramatsu, K., Araki, T., Ueda, S., Tamamura, H., Otaka, A., Kusano, S., Terakubo, S., Nakashima, H., et al. (2003). Molecular-size reduction of a potent CXCR4-chemokine antagonist using orthogonal combination

of conformation- and sequence-based libraries. Angew. Chem. Int. Ed. Engl. *42*, 3251–3253.

Futaki, S. (2006). Oligoarginine vectors for intracellular delivery: design and cellular-uptake mechanisms. Biopolymers *84*, 241–249.

Futaki, S., Suzuki, T., Ohashi, W., Yagami, T., Tanaka, S., Ueda, K., and Sugiura, Y. (2001). Arginine-rich peptides. An abundant source of membrane-permeable peptides having potential as carriers for intracellular protein delivery. J. Biol. Chem. *276*, 5836–5840.

Gerbal-Chaloin, S., Gondeau, C., Aldrian-Herrada, G., Heitz, F., Gauthier-Rouvière, C., and Divita, G. (2007). First step of the cell-penetrating peptide mechanism involves Rac1 GTPase-dependent actin-network remodelling. Biol. Cell *99*, 223–238.

Hamon, M., Mbemba, E., Charnaux, N., Slimani, H., Brule, S., Saffar, L., Vassy, R., Prost, C., Lievre, N., Starzec, A., and Gattegno, L. (2004). A syndecan-4/CXCR4 complex expressed on human primary lymphocytes and macrophages and HeLa cell line binds the CXC chemokine stromal cell-derived factor-1 (SDF-1). Glycobiology *14*, 311–323.

Ishihara, M. (1993). Biosynthesis, structure, and biological activity of basic FGF binding domains of heparan sulfate. Trends Glycosci. Glycotechnol. *5*, 343–354.

Kimpton, J., and Emerman, M. (1992). Detection of replication-competent and pseudotyped human immunodeficiency virus with a sensitive cell line on the basis of activation of an integrated β-galactosidase gene. J. Virol. *66*, 2232–2239.

Kodama, E.I., Kohgo, S., Kitano, K., Machida, H., Gatanaga, H., Shigeta, S., Matsuoka, M., Ohrui, H., and Mitsuya, H. (2001). 4′-ethynyl nucleoside analogs: potent inhibitors of multidrug-resistant human immunodeficiency virus variants in vitro. Antimicrob. Agents Chemother. *45*, 1539–1546.

Kosuge, M., Takeuchi, T., Nakase, I., Jones, A.T., and Futaki, S. (2008). Cellular internalization and distribution of arginine-rich peptides as a function of extracellular peptide concentration, serum, and plasma membrane associated proteoglycans. Bioconjug. Chem. *19*, 656–664.

Koyanagi, Y., Harada, S., Takahashi, M., Uchino, F., and Yamamoto, N. (1985). Selective cytotoxicity of AIDS virus infection towards HTLV-I-transformed cell lines. Int. J. Cancer *36*, 445–451.

Letoha, T., Keller-Pintér, A., Kusz, E., Kolozsi, C., Bozsó, Z., Tóth, G., Vizler, C., Oláh, Z., and Szilák, L. (2010). Cell-penetrating peptide exploited syndecans. Biochim. Biophys. Acta *1798*, 2258–2265.

Maréchal, V., Prevost, M.-C., Petit, C., Perret, E., Heard, J.-M., and Schwartz, O. (2001). Human immunodeficiency virus type 1 entry into macrophages mediated by macropinocytosis. J. Virol. *75*, 11166–11177.

Meier, O., Boucke, K., Hammer, S.V., Keller, S., Stidwill, R.P., Hemmi, S., and Greber, U.F. (2002). Adenovirus triggers macropinocytosis and endosomal leakage together with its clathrin-mediated uptake. J. Cell Biol. *158*, 1119–1131.

Mercer, J., and Helenius, A. (2008). Vaccinia virus uses macropinocytosis and apoptotic mimicry to enter host cells. Science *320*, 531–535.

Mercer, J., and Helenius, A. (2009). Virus entry by macropinocytosis. Nat. Cell Biol. *11*, 510–520.

Mitola, S., Sozzani, S., Luini, W., Primo, L., Borsatti, A., Weich, H., and Bussolino, F. (1997). Tat-human immunodeficiency virus-1 induces human monocyte chemotaxis by activation of vascular endothelial growth factor receptor-1. Blood *90*, 1365–1372.

Möhle, R., Bautz, F., Denzlinger, C., and Kanz, L. (2001). Transendothelial migration of hematopoietic progenitor cells. Role of chemotactic factors. Ann. N Y Acad. Sci. *938*, 26–34, discussion 34–35.

Nakase, I., Niwa, M., Takeuchi, T., Sonomura, K., Kawabata, N., Koike, Y., Takehashi, M., Tanaka, S., Ueda, K., Simpson, J.C., et al. (2004). Cellular uptake of arginine-rich peptides: roles for macropinocytosis and actin rearrangement. Mol. Ther. *10*, 1011–1022.

Nakase, I., Tadokoro, A., Kawabata, N., Takeuchi, T., Katoh, H., Hiramoto, K., Negishi, M., Nomizu, M., Sugiura, Y., and Futaki, S. (2007). Interaction of arginine-rich peptides with membrane-associated proteoglycans is crucial for induction of actin organization and macropinocytosis. Biochemistry *46*, 492–501.

Nakase, I., Hirose, H., Tanaka, G., Tadokoro, A., Kobayashi, S., Takeuchi, T., and Futaki, S. (2009). Cell-surface accumulation of flock house virus-derived peptide leads to efficient internalization via macropinocytosis. Mol. Ther. *17*, 1868–1876.

Nakashima, H., Hashimoto, M., Sadakane, Y., Tomohiro, T., and Hatanaka, Y. (2006). Simple and versatile method for tagging phenyldiazirine photophores. J. Am. Chem. Soc. *128*, 15092–15093.

Orsini, M.J., Parent, J.L., Mundell, S.J., Marchese, A., and Benovic, J.L. (1999). Trafficking of the HIV coreceptor CXCR4. Role of arrestins and identification of residues in the C-terminal tail that mediate receptor internalization. J. Biol. Chem. *274*, 31076–31086.

Phillips, R., and Ager, A. (2002). Activation of pertussis toxin-sensitive CXCL12 (SDF-1) receptors mediates transendothelial migration of T lymphocytes across lymph node high endothelial cells. Eur. J. Immunol. *32*, 837–847.

Rey, M., Valenzuela-Fernández, A., Urzainqui, A., Yáñez-Mó, M., Pérez-Martínez, M., Penela, P., Mayor, F., Jr., and Sánchez-Madrid, F. (2007). Myosin IIA is involved in the endocytosis of CXCR4 induced by SDF-1α. J. Cell Sci. *120*, 1126–1133.

Rubio Demirovic, A., Canadi, J., Weiglhofer, W., Scheidegger, P., Jaussi, R., and Kurt, B.-H. (2003). HIV TAT basic peptide is not a high-affinity ligand for VEGF receptor 2. Biol. Chem. *384*, 1435–1441.

Schaeffer, E., Geleziunas, R., and Greene, W.C. (2001). Human immunodeficiency virus type 1 Nef functions at the level of virus entry by enhancing cytoplasmic delivery of virions. J. Virol. *75*, 2993–3000.

Schramm, B., Penn, M.L., Speck, R.F., Chan, S.Y., De Clercq, E., Schols, D., Connor, R.I., and Goldsmith, M.A. (2000). Viral entry through CXCR4 is a pathogenic factor and therapeutic target in human immunodeficiency virus type 1 disease. J. Virol. *74*, 184–192.

Signoret, N., Oldridge, J., Pelchen-Matthews, A., Klasse, P.J., Tran, T., Brass, L.F., Rosenkilde, M.M., Schwartz, T.W., Holmes, W., Dallas, W., et al. (1997). Phorbol esters and SDF-1 induce rapid endocytosis and down modulation of the chemokine receptor CXCR4. J. Cell Biol. *139*, 651–664.

Swanson, J.A., and Watts, C. (1995). Macropinocytosis. Trends Cell Biol. *5*, 424–428.

Tamamura, H., Otaka, A., and Fujii, N. (2005). Development of anti-HIV agents targeting dynamic supramolecular mechanism: entry and fusion inhibitors based on CXCR4/CCR5 antagonists and gp41-C34-remodeling peptides. Curr. HIV Res. *3*, 289–301.

Tkachenko, E., Lutgens, E., Stan, R.-V., and Simons, M. (2004). Fibroblast growth factor 2 endocytosis in endothelial cells proceed via syndecan-4-dependent activation of Rac1 and a Cdc42-dependent macropinocytic pathway. J. Cell Sci. *117*, 3189–3199.

Tomohiro, T., Hashimoto, M., and Hatanaka, Y. (2005). Cross-linking chemistry and biology: development of multifunctional photoaffinity probes. Chem. Rec. *5*, 385–395.

Venkatesan, S., Rose, J.J., Lodge, R., Murphy, P.M., and Foley, J.F. (2003). Distinct mechanisms of agonist-induced endocytosis for human chemokine receptors CCR5 and CXCR4. Mol. Biol. Cell *14*, 3305–3324.

Voermans, C., Anthony, E.C., Mul, E., van der Schoot, E., and Hordijk, P. (2001). SDF-1-induced actin polymerization and migration in human hematopoietic progenitor cells. Exp. Hematol. *29*, 1456–1464.

Wadia, J.S., Stan, R.V., and Dowdy, S.F. (2004). Transducible TAT-HA fusogenic peptide enhances escape of TAT-fusion proteins after lipid raft macropinocytosis. Nat. Med. *10*, 310–315.

Wang, J.-H., Wells, C., and Wu, L. (2008). Macropinocytosis and cytoskeleton contribute to dendritic cell-mediated HIV-1 transmission to $CD4^+$ T cells. Virology *381*, 143–154.

Wender, P.A., Galliher, W.C., Goun, E.A., Jones, L.R., and Pillow, T.H. (2008). The design of guanidinium-rich transporters and their internalization mechanisms. Adv. Drug Deliv. Rev. *60*, 452–472.

Wu, Y., and Yoder, A. (2009). Chemokine coreceptor signaling in HIV-1 infection and pathogenesis. PLoS Pathog. *5*, e1000520.

Xiao, H., Neuveut, C., Tiffany, H.L., Benkirane, M., Rich, E.A., Murphy, P.M., and Jeang, K.T. (2000). Selective CXCR4 antagonism by Tat: implications for in vivo expansion of coreceptor use by HIV-1. Proc. Natl. Acad. Sci. USA *97*, 11466–11471.

Yano, Y., Yano, A., Oishi, S., Sugimoto, Y., Tsujimoto, G., Fujii, N., and Matsuzaki, K. (2008). Coiled-coil tag–probe system for quick labeling of membrane receptors in living cells. ACS Chem. Biol. *3*, 341–345.

Yoder, A., Yu, D., Dong, L., Iyer, S.R., Xu, X., Kelly, J., Liu, J., Wang, W., Vorster, P.J., Agulto, L., et al. (2008). HIV envelope-CXCR4 signaling activates cofilin to overcome cortical actin restriction in resting CD4 T cells. Cell *134*, 782–792.

Zhang, W.-B., Navenot, J.-M., Haribabu, B., Tamamura, H., Hiramatu, K., Omagari, A., Pei, G., Manfredi, J.P., Fujii, N., Broach, J.R., and Peiper, S.C. (2002). A point mutation that confers constitutive activity to CXCR4 reveals that T140 is an inverse agonist and that AMD3100 and ALX40-4C are weak partial agonists. J. Biol. Chem. *277*, 24515–24521.

Bioorganic & Medicinal Chemistry 21 (2013) 2079–2087

Contents lists available at SciVerse ScienceDirect

Bioorganic & Medicinal Chemistry

journal homepage: www.elsevier.com/locate/bmc

Design and synthesis of biotin- or alkyne-conjugated photoaffinity probes for studying the target molecules of PD 404182

Tsukasa Mizuhara [a], Shinya Oishi [a,*], Hiroaki Ohno [a], Kazuya Shimura [b], Masao Matsuoka [b], Nobutaka Fujii [a,*]

[a] Graduate School of Pharmaceutical Sciences, Kyoto University, Sakyo-ku, Kyoto 606-8501, Japan
[b] Institute for Virus Research, Kyoto University, Sakyo-ku, Kyoto 606-8507, Japan

ARTICLE INFO

Article history:
Received 12 December 2012
Revised 5 January 2013
Accepted 5 January 2013
Available online 16 January 2013

Keywords:
Anti-HIV agents
PD 404182
Photoaffinity labeling
Pyrimidobenzothiazine

ABSTRACT

To investigate the mechanism of action of the potent antiviral compound PD 404182, three novel photoaffinity probes equipped with a biotin or alkyne indicator were designed and synthesized based on previous structure–activity relationship studies. These probes retained the potent anti-HIV activity of the original pyrimidobenzothiazine derivatives. In photoaffinity labeling studies using HIV-1-infected H9 cells (H9IIIB), eight potential proteins were observed to bind PD 404182.

1. Introduction

3,4-Dihydro-2*H*,6*H*-pyrimido[1,2-*c*][1,3]benzothiazin-6-imine (PD 404182) (**1**)[1–3] is a potent antiviral agent against the human immunodeficiency virus (HIV) and the hepatitis C virus (HCV) (Fig. 1).[4,5] In structure–activity relationship (SAR) studies[5,6] of compound **1** using a series of facile synthetic procedures,[7,8] we identified several derivatives **2–4** that exhibited two- or three-fold more potent anti-HIV activity than compound **1**. The comparative time of drug addition study using standard anti-HIV agents demonstrated that compound **1** showed a similar antiviral profile against HIV-1_{IIIB} infection with that of DS 5000 (adsorption inhibitor)[9] and enfuvirtide (fusion inhibitor),[10] indicating that compound **1** impaired virus replication at the early-stage of HIV infection.[5] Additionally, the antiviral activities of compound **1** against multiple HIV clades suggest that the target molecule of compound **1** is not chemokine receptors (CC chemokine receptor type 5[11] or CXC chemokine receptor type 4[12]).[5] Recently, the virucidal effects of compound **1** against HCV, HIV and the simian immunodeficiency virus have also been reported.[13] However, the mode of action and mechanism of antiviral activity of compound **1** has not yet been fully elucidated.

Photoaffinity labeling is an efficient approach to identify the target protein(s) of biologically active molecules.[14] In modern drug discovery, there have been a number of successful examples that have determined the target molecules and identified the binding site through the formation of a covalent bond between the ligand and the specific protein.[15] In general, photoaffinity probes contain three functional groups: a bioactive scaffold, a photoreactive group and an indicator group. A biotin-tag is widely employed as an indicator because biotinylated proteins can be detected and isolated by several immunological methods or through a biotin-avidin interaction.[16] A terminal alkyne is an alternative indicator for Huisgen cycloaddition-mediated conjugation with various azide-modified reporters, such as fluorescent-azide and biotin-azide after the crosslinking reaction onto the target protein(s).[17]

In this article, the design and synthesis of biotin- or alkyne-conjugated photoaffinity probes based on previous SAR studies, and its application for photoaffinity labeling studies are described.

2. Results and discussion

2.1. Design of biotin- or alkyne-conjugated photoaffinity probes from PD 404182

Trifunctional probes for the target protein(s) of compound **1** and the derivatives were designed on the basis of our previous SAR investigations.[5,6] In our previous study, the introduction of a hydrophobic group on the benzene ring and the cyclic amidine

Abbreviations: MAGI, multinuclear activation of a galactosidase indicator.

* Corresponding authors. Tel.: +81 75 753 4551; fax: +81 75 753 4570.
E-mail addresses: soishi@pharm.kyoto-u.ac.jp (S. Oishi), nfujii@pharm.kyoto-u.ac.jp (N. Fujii).

0968-0896/$ - see front matter © 2013 Elsevier Ltd. All rights reserved.
http://dx.doi.org/10.1016/j.bmc.2013.01.016

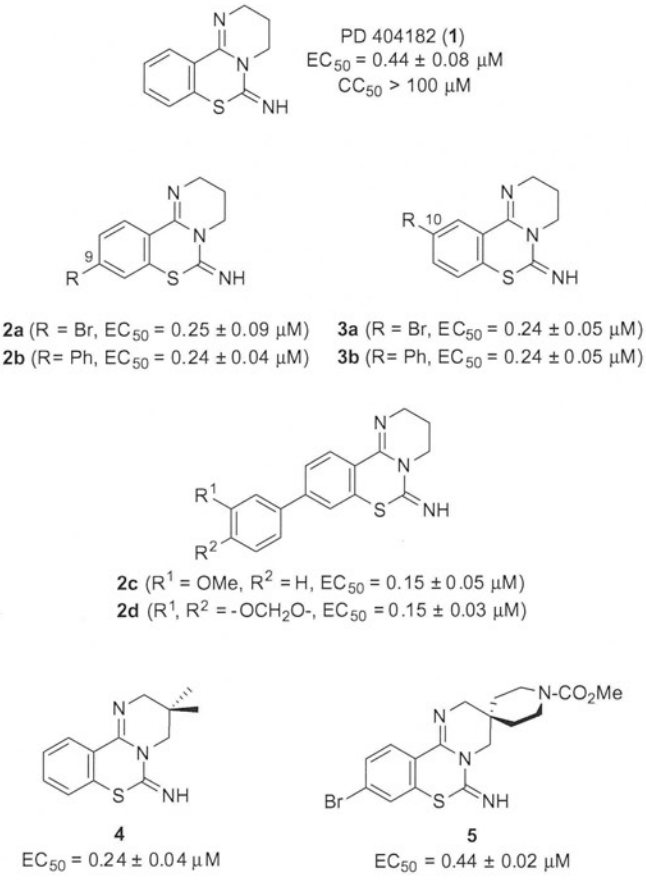

Figure 1. Structures and anti-HIV activity of PD 404182 and the derivatives **2–5**.

substructures effectively improved antiviral activity (compounds **2–4**, Fig. 1). We expected that these moieties would potentially take part in a favorable interaction(s) with the target molecule(s), and the incorporation of a hydrophobic and photoreactive benzophenone group on the pyrimidobenzothiazine scaffold would be tolerated. Additionally, the *N*-alkoxycarbonyl piperidine group onto the amidine substructure of **1** reproduced potent anti-HIV activity (compound **5**), indicating that this part could be used as a linkage position for the addition of functional groups.

With this in mind, we designed three photoaffinity probes. Compound **6** was modified with indicator biotin via a photoreactive benzophenone group onto the benzene ring substructure (Fig. 2). Compound **7** equips the biotin and benzophenone groups on the right-part amidine moiety. The biotin moiety is conjugated with benzophenone via a polyethylene glycol (PEG) linker as the spacer. Compound **8** is an alkyne-containing derivative.

2.2. Synthesis of biotin-conjugated probe 6

Synthesis of the probe **6** started with the preparation of benzophenone boronic acid pinacol ester **11** (Scheme 1). Condensation of *p*-(hydroxymethyl)benzoic acid **9** and *N,O*-dimethylhydroxylamine followed by TBDPS protection of a primary hydroxy group gave an amide **10**. Subsequent nucleophilic addition of an in situ-generated organolithium compound easily provided the desired boronate **11**.[18]

We next assembled the components to synthesize the biotin-conjugated probe **6** (Scheme 1). Alkylation of compound **2a** with *p*-methoxybenzyl (PMB) bromide followed by Suzuki–Miyaura cross coupling with compound **11** afforded a benzophenone-conjugated pyrimidobenzothiazine **13**. Desilylation of **13** and the subsequent reaction with *p*-nitrophenyl chloroformate afforded the carbonate **16**. The biotin moiety was incorporated by reaction of **16** with biotin-PEG-NH_2 (**15**), which was prepared by catalytic hydrogenation of azide **14**.[19] TFA-mediated deprotection of the PMB group in compound **17** provided the desired probe **6**.

2.3. Synthesis of biotin-conjugated probe 7

Synthesis of the biotin-conjugated probe **7** is outlined in Scheme 2. PMB protection of compound **18**[6] followed by selective removal of the PMB group on the piperidine ring provided compound **20**. Separately, the synthesis of biotin-benzophenone adduct **23** started from 4-(*tert*-butyldiphenylsilyloxy)methyl-4′-(hydroxymethyl)benzophenone **21**.[20] The treatment of **21** with

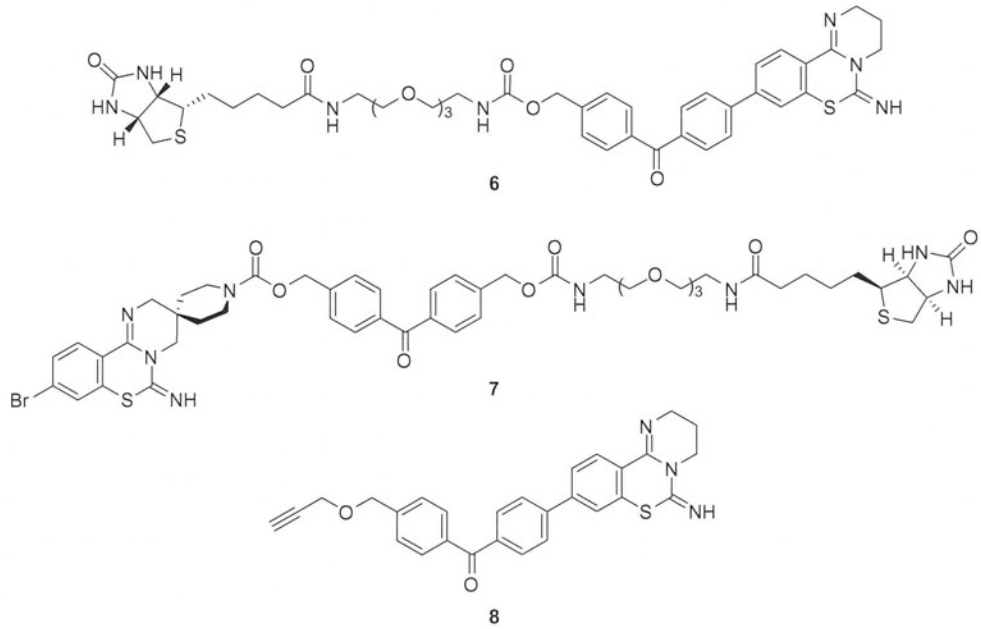

Figure 2. Structures of photoaffinity probes **6–8**.

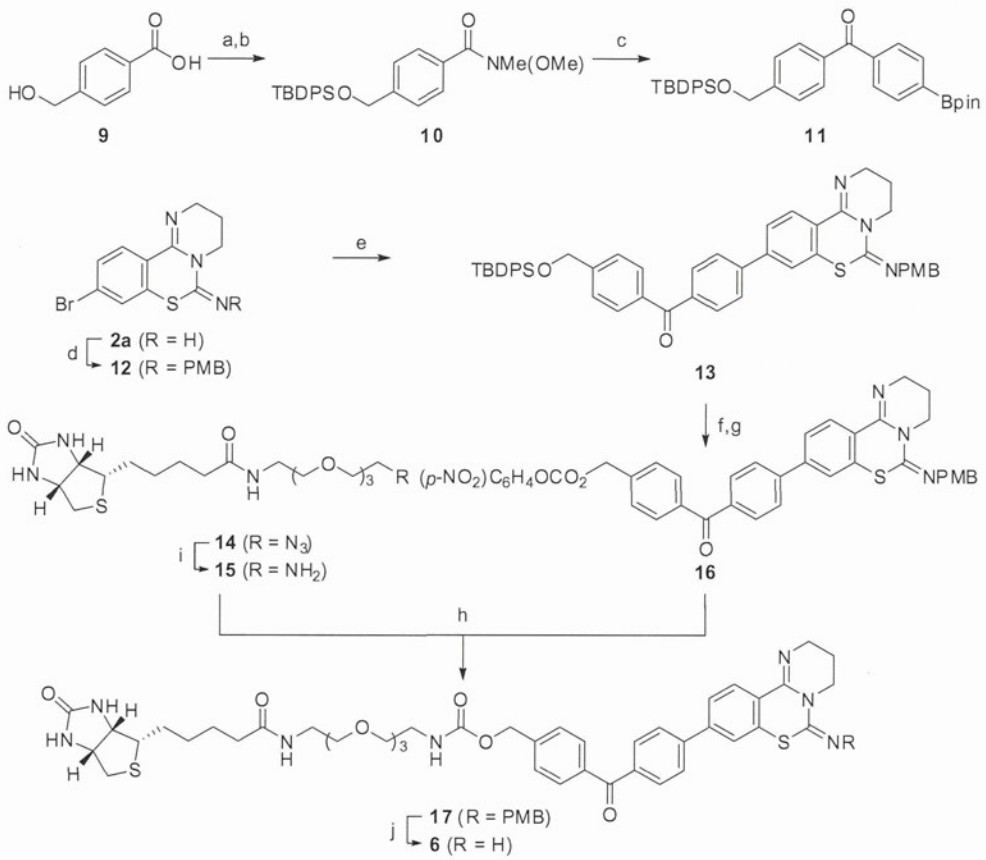

Scheme 1. Synthesis of biotin-conjugated probe **6**. Reagents and conditions: (a) HNMe(OMe)·HCl, EDC·HCl, HOBt·H_2O, Et_3N, DMF, rt; (b) TBDPSCl, Et_3N, DMAP, CH_2Cl_2, rt, 49% [2 steps (a,b)]; (c) 2-(4-bromophenyl)-4,4,5,5-tetramethyl-1,3,2-dioxaborolane, *t*-BuLi, THF, pentane, −78 to rt, 83%; (d) *t*-BuOK, DMF, 0 °C, then PMBBr, rt, 98%; (e) **11**, $Pd(PPh_3)_4$, $PdCl_2(dppf)\cdot CH_2Cl_2$, K_2CO_3, toluene, EtOH, H_2O, reflux, 96%; (f) TBAF, THF, rt; (g) *p*-nitrophenyl chloroformate, pyridine, CH_2Cl_2, reflux; (h) Et_3N, DMF, rt to 40 °C, 46% [3 steps (f–h)]; (i) H_2, 10% Pd-C, MeOH, rt; (j) MS4Å, TFA, $CHCl_3$, rt, 35%.

chloroformate furnished a carbonate **22**. Biotin-PEG-NH_2 **15** was successfully conjugated onto **22** to give the biotin-benzophenone adduct **23**. Desilylation of **23**, treatment with *p*-nitrophenyl chloroformate and coupling with **20** provided biotin/benzophenone-conjugated **26**. PMB deprotection of **26** afforded the desired probe **7**.

2.4. Synthesis of alkyne-containing probe 8

We next investigated the synthesis of alkyne-containing probe **8** (Scheme 3). Suzuki–Miyaura cross coupling of compound **27**[5] with boronate **11** gave compound **28**. Subsequent modifications including desilylation, propargylation, and removal of the *tert*-butyl group provided the expected alkyne-conjugated probe **8**.

2.5. Anti-HIV activity of biotin- or alkyne-conjugated probes

The antiviral activities of probes **6–8** against HIV-1_{IIIB} were measured by multinuclear activation of a galactosidase indicator (MAGI) assay. In this assay, the inhibitory activity against HIV infection at the early stage, including virus attachment and membrane fusion to host cells, can be evaluated.[21] Both biotin-conjugated probes **6** and **7** showed potent anti-HIV activity with EC_{50} values of 6.87 and 5.11 μM, respectively (Table 1). These activities were slightly lower than that of compound **1**; however, the incorporation of large functional groups including benzophenone, the PEG linker and the biotinyl reporter was largely tolerated. Alkyne-conjugated probe **8** potently inhibited HIV infection (EC_{50} = 0.64 μM). These probes **6–8** represent promising tools for the identification of the target molecule(s) of compound **1** and the derivatives.

2.6. Photoaffinity labeling experiment using biotin-conjugated probes for HIV-1-infected H9 cells

Probes **6** and **7** were applied to the experiment for target identification of compound **1** and the derivatives. After HIV-1-infected H9 cells (H9IIIB) were incubated with a probe (**6** or **7**) for 1 h, the cells were exposed to UV–vis light (>300 nm) for 1 min. After cell lysis, the biotinylated proteins were captured with NeutrAvidin agarose beads. The whole was subjected to separation by SDS–PAGE followed by Western blot analysis.

Eight bands of 95, 80, 75, 70, 60, 55, 48 and 40 kDa proteins were observed from the cell samples incubated with probe **6** (Lane A, Fig. 3). These bands were competed by unlabeled compound **3a**, suggesting that the labeling was PD 404182-specific (Lane C). In contrast, these bands, with the exception of the 70 and 40 kDa bands, were not detected in the cells incubated with probe **7** (Lane B). This observation indicated that the potential target proteins did not fully interact with the benzophenone group on the right-part amidine moiety in the pyrimidobenzothiazine scaffold of **7**.

This preliminary experiment demonstrated that the synthesized probe **6** could be useful for the identification of the target protein(s) of compound **1**. Efforts of the crosslinking experiments using alkyne-conjugated probe **8** are also currently in progress.

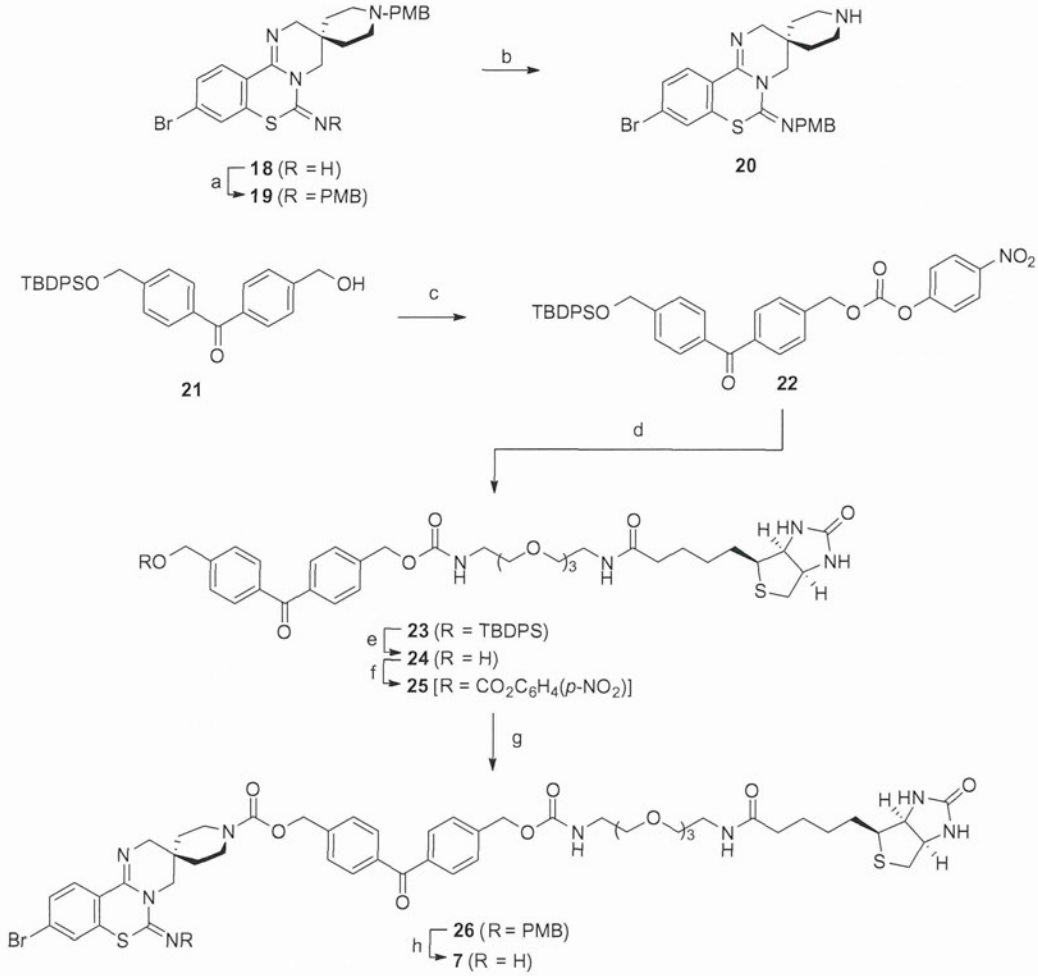

Scheme 2. Synthesis of biotin-conjugated probe **7**. Reagents and conditions: (a) *t*-BuOK, DMF, 0 °C, then PMBBr, rt, 81%; (b) 1-chloroethyl chloroformate, Et_3N, CH_2Cl_2, 0 °C, then MeOH, reflux; (c) 4-nitrophenyl chloroformate, pyridine, CH_2Cl_2, reflux; (d) **15**, Et_3N, DMF, rt, quant. [2 steps (c,d)]; (e) HF-pyridine, THF, 0 °C to rt, 73%; (f) 4-nitrophenyl chloroformate, pyridine, CH_2Cl_2, reflux, 80%; (g) **20**, Et_3N, DMF, rt; (h) MS4Å, TFA, $CHCl_3$, rt, 36% [2 steps (g,h)].

3. Conclusions

In conclusion, we have designed and synthesized novel photoaffinity probes of antiviral PD 404182 with photoreactive benzophenone, and biotin or alkyne indicators. The probes exhibited equipotent or slightly less potent anti-HIV activities when compared with the activity of the parent compound **1**. Preliminary photoaffinity labeling experiments suggest that these probes could be useful in the identification of a potential target protein(s), the binding site on the target protein(s) and the mechanism(s) of action of PD 404182 derivatives.

4. Experimental

4.1. Synthesis

4.1.1. General methods

^1H NMR spectra were recorded using a JEOL AL-400 or a JEOL ECA-500 spectrometer. Chemical shifts are reported in δ (ppm) relative to Me_4Si ($CDCl_3$) or DMSO (DMSO-d_6) as internal standards. ^{13}C NMR spectra were referenced to the residual solvent signal. Exact mass (HRMS) spectra were recorded on a JMS-HX/HX 110A mass spectrometer. Melting points were measured by a hot stage melting point apparatus (uncorrected). For flash chromatography, Wakogel C-300E (Wako) or aluminum oxide 90 standardized (Merck) were employed. For preparative TLC, TLC silica gel 60 F_{254} (Merck) or TLC aluminum oxide 60 F_{254} basic (Merck) were employed. For analytical HPLC, a Cosmosil 5C18-ARII column (4.6 × 250 mm, Nacalai Tesque, Inc., Kyoto, Japan) was employed with a linear gradient of CH_3CN containing 0.1% (v/v) NH_3 at a flow rate of 1 mL/min on a Shimadzu LC-10ADvp (Shimadzu Corp., Ltd, Kyoto, Japan), and eluting products were detected by UV at 254 nm. Preparative HPLC was performed using a COSMOSIL 5C18-ARII column (20 × 250 mm, Nacalai Tesque Inc.) with a linear gradient of MeCN containing 0.1% (v/v) NH_3 at a flow rate of 8 mL/min on Shimadzu LC-6AD (Shimadzu corporation, Ltd). The purity of the compounds **6–8** was determined by HPLC analysis as >95%.

4.1.2. 4-[(*tert*-Butyldiphenylsilyloxy)methyl]-*N*-methoxy-*N*-methylbenzamide (10)

To a mixture of 4-(hydroxymethyl)benzoic acid **9** (4.6 g, 30.0 mmol), *N*,*O*-dimethylhydroxylamine hydrochloride (14.6 g, 150.0 mmol), Et_3N (21.7 mL, 150.0 mmol) in DMF (300 mL) were added EDC·HCl (11.5 g, 60.0 mmol) and HOBt·H_2O (9.2 g, 60.0 mmol). After being stirred at rt overnight, solvent was evaporated. The residue was dissolved in EtOAc, and washed with 1 N HCl, satd $NaHCO_3$, brine, and dried over $MgSO_4$. The filtrate was

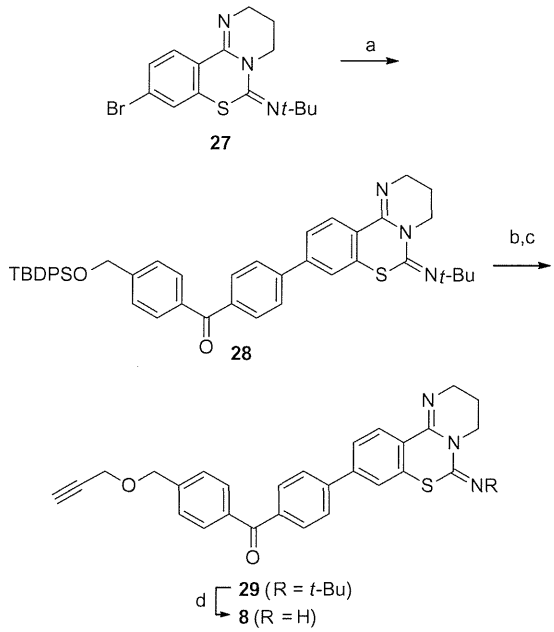

Scheme 3. Synthesis of alkyne-conjugated probe **8**. Reagents and conditions: (a) **11**, $Pd(PPh_3)_4$, $PdCl_2(dppf)\cdot CH_2Cl_2$, K_2CO_3, toluene, EtOH, H_2O, reflux, 71%; (b) TBAF, THF, rt; (c) NaH, THF, propargyl bromide, 0 °C to rt, 60% [2 steps (b,c)]; (d) MS4Å, TFA, $CHCl_3$, reflux, 92%.

Table 1
Anti-HIV activities of the probes **6–8**

Compound	EC_{50}[a] (μM)
PD 404182[5]	0.44 ± 0.08
6	6.87 ± 2.22
7	5.11 ± 1.31
8	0.64 ± 0.06

[a] EC_{50} values represent the concentration of compound required to inhibit the HIV-1 infection by 50%, and were obtained from three independent experiments.

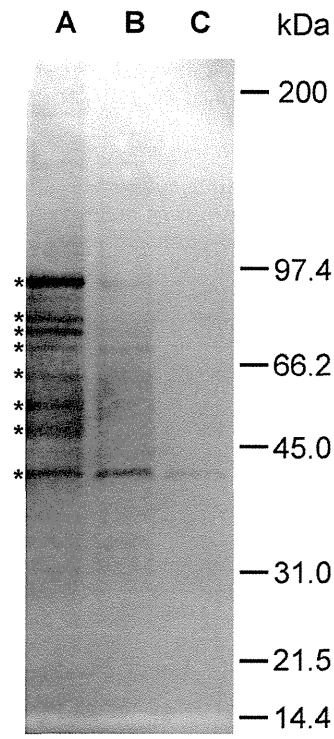

Figure 3. Western blot analysis of the photolabeled proteins with biotin-conjugated probes **6** and **7**. H9IIIB cells were incubated with (A) 20 μM probe **6**, (B) 20 μM probe **7**, and (C) 20 μM probe **6** and 40 μM compound **3a**. The cells were exposed to UV light for 1 min and were lysed. The resulting photolabeled proteins were captured onto NeutrAvidin-agarose and the whole was subjected to SDS–PAGE. The resulting gel was analyzed by Western blotting with streptavidin–HRP.

concentrated to give crude Weinreb amide (4.05 g, ca. 20.7 mmol). To the mixture of the Weinreb amide, a solution of Et_3N (8.98 mL, 62.1 mmol) and DMAP (252.9 mg, 2.1 mmol) in CH_2Cl_2 (138 mL) was slowly added TBDPSCl (5.83 mL, 22.8 mmol). After being stirred at rt for 3 h, the reaction mixture was quenched with water. After concentration, the residue was dissolved in EtOAc. The mixture was washed with satd $NaHCO_3$, brine, and dried over $MgSO_4$. After concentration, the residue was purified by flash column chromatography over silica gel with *n*-hexane/EtOAc (3:1) to give the title compound **10** as colorless oil (6.98 g, 49%): IR (neat) cm^{-1}: 1644 (C=O); ^1H NMR (400 MHz, $CDCl_3$) δ: 1.10 (s, 9H, 3 × CH_3), 3.36 (s, 3H, CH_3), 3.57 (s, 3H, CH_3), 4.80 (s, 2H, CH_2), 7.36–7.43 (m, 8H, Ar), 7.65–7.70 (m, 6H, Ar); ^{13}C NMR (100 MHz, $CDCl_3$) δ: 19.3, 26.8 (3C), 33.8, 61.0, 65.2, 125.4 (2C), 127.7 (4C), 128.2 (2C), 129.8 (2C), 132.6, 133.3 (2C), 135.5 (4C), 143.8, 169.9; HRMS (FAB): *m/z* calcd for $C_{26}H_{32}NO_3Si$ $[M+H]^+$ 434.2152; found: 434.2160.

4.1.3. 4-[(*tert*-Butyldiphenylsilyloxy)methyl]-4′-(4,4,5,5-tetramethyl-1,3,2-dioxaborolan-2-yl)benzophenone (11)

To a solution of 1,4-dibromobenzene (3.13 g, 13.3 mmol) and 2-isopropoxy-4,4,5,5-tetramethyl-1,3,2-dioxaborolane (2.80 mL, 13.8 mmol) in anhydrous THF (60 mL) was added *t*-BuLi (19.4 mL, 1.55 M in pentane, 30.0 mmol) dropwise over 3 min at −78 °C under an Ar atmosphere. After being stirred at −78 °C for 30 min, additional *t*-BuLi (19.4 mL, 1.55 M in pentane, 30.0 mmol) was added dropwise over 3 min. After being stirred at the same temperature for additional 20 min, compound **10** (3.25 g, 7.5 mmol) was added. The reaction mixture was warmed to rt over 1 h and quenched with satd NH_4Cl. The whole was extracted with EtOAc and the extract was dried over $MgSO_4$. After concentration, the residue was purified by silica gel chromatography with *n*-hexane/EtOAc (9:1) to give the title compound **11** as yellow oil (3.60 g, 83%): IR (neat) cm^{-1}: 1659 (C=O); ^1H NMR (400 MHz, $CDCl_3$) δ: 1.11 (s, 9H, 3 × CH_3), 1.37 (s, 12H, 4 × CH_3), 4.85 (s, 2H, CH_2), 7.37–7.46 (m, 8H, Ar), 7.69 (d, J = 6.6 Hz, 4H, Ar), 7.75–7.80 (m, 4H, Ar), 7.92 (d, J = 8.0 Hz, 2H, Ar); ^{13}C NMR (100 MHz, $CDCl_3$) δ: 19.3, 24.8 (4C), 26.8 (3C), 65.2, 84.2 (2C), 125.6 (2C), 127.8 (4C), 128.9 (2C), 129.8 (2C), 130.2 (2C), 133.2 (2C), 134.5 (2C), 134.8, 135.5 (4C), 136.2, 140.0, 146.0, 196.6; HRMS (FAB): *m/z* calcd for $C_{36}H_{42}BO_4Si$ $[M+H]^+$ 577.2945; found: 577.2949.

4.1.4. 9-Bromo-3,4-dihydro-*N*-(*p*-methoxybenzyl)-2*H*,6*H*-pyrimido[1,2-*c*][1,3]benzothiazin-6-imine (12)

To the flask containing **2a** (740.4 mg, 2.50 mmol) and *t*-BuOK (561.1 mg, 5.00 mmol) was added DMF (10.0 mL) at 0 °C under an Ar atmosphere. After being stirred at the same temperature for 30 min, PMB-Br (729.0 μL, 5.00 mmol) was added. After being stirred at rt for 1 h, the reaction mixture was quenched with H_2O. The whole was extracted with EtOAc, and washed with satd $NaHCO_3$, brine, and dried over $MgSO_4$. After concentration, the residue was purified by flash column chromatography over aluminum oxide with *n*-hexane/EtOAc (3:1) to give the title compound **12** as pale yellow amorphous (1.02 g, 98%): IR (neat) cm^{-1}: 1661 (C=N), 1510 (C=N); ^1H NMR (400 MHz, $CDCl_3$) δ: 1.97-2.03 (m, 2H), 3.64 (t, J = 5.7 Hz, 2H, CH_2), 3.80-3.84 (m, 5H, OCH_3, CH_2), 4.14 (s, 2H, CH_2), 6.86 (d, J = 8.5 Hz, 2H, Ar), 7.21-7.27 (m, 3H, Ar), 7.38 (dd,

J = 8.2, 1.8 Hz, 1H, Ar), 7.43 (d, J = 1.8 Hz, 1H, Ar); ^{13}C NMR (100 MHz, $CDCl_3$) δ: 19.8, 38.7, 44.3, 47.7, 55.3, 111.9, 114.1 (2C), 124.8, 127.9, 129.5, 130.2, 130.3 (2C), 132.6, 133.4, 138.7, 147.6, 159.1; HRMS (FAB): m/z calcd for $C_{19}H_{19}N_3OS$ $[M+H]^+$ 416.0432; found: 416.0431.

4.1.5. 9-{4-[4-(*tert*-Butyldiphenylsilyloxy)methyl]-benzoylphenyl}-3,4-dihydro-*N*-(*p*-methoxybenzyl)-2*H*,6*H*-pyrimido[1,2-*c*][1,3]benzothiazin-6-imine (13)

$Pd(PPh_3)_4$ (32.8 mg, 4 mol %) and $PdCl_2(dppf)\cdot CH_2Cl_2$ (17.4 mg, 3 mol %) were added to a solution of **12** (296.2 mg, 0.71 mmol) and **11** (409.4 mg, 0.71 mmol) in toluene (7.1 mL)-EtOH (4.3 mL)-1 M aq K_2CO_3 (7.1 mL). After being stirred at reflux for 1 h, the mixture was extracted with $CHCl_3$. The extract was dried over $MgSO_4$ and concentrated. The residue was purified by flash chromatography over aluminum oxide with *n*-hexane/EtOAc (1:0 to 9:1) to give the title compound **13** as pale yellow amorphous (536.2 mg, 96%): IR (neat) cm^{-1}: 1658 (C=O), 1607 (C=N), 1511 (C=N); ^{1}H NMR (400 MHz, $CDCl_3$) δ: 1.12 (s, 9H, 3 × CH_3), 2.03–2.08 (m, 2H), 3.70 (t, J = 5.5 Hz, 2H, CH_2), 3.77 (s, 3H, CH_3), 3.88 (t, J = 5.9 Hz, 2H, CH_2), 4.19 (s, 2H, CH_2), 4.86 (s, 2H, CH_2), 6.84 (d, J = 8.5 Hz, 2H, Ar), 7.28 (m, 1H, Ar), 7.38–7.56 (m, 14H, Ar), 7.71 (dd, J = 7.6, 1.2 Hz, 4H, Ar), 7.81 (d, J = 8.0 Hz, 2H, Ar), 7.86 (d, J = 8.0 Hz, 2H, Ar); ^{13}C NMR (125 MHz, $CDCl_3$) δ: 19.3, 19.8, 26.8 (3C), 39.0, 44.3, 47.7, 55.2, 65.1, 112.2, 113.9 (2C), 125.6 (2C), 125.7, 127.0 (2C), 127.7 (4C), 128.7, 129.5, 129.8 (2C), 130.1 (2C), 130.2, 130.3 (2C), 130.5 (2C), 133.1 (2C), 135.0, 135.5 (4C), 136.2, 136.4, 137.0, 142.1, 143.5, 146.0, 148.2, 158.9, 195.8; HRMS (FAB): m/z calcd for $C_{49}H_{48}N_3O_3SSi$ $[M+H]^+$ 786.3186; found: 786.3178.

4.1.6. *N*-(2-[2-{2-(2-Aminoethoxy)ethoxy}ethoxy]ethyl)-5-[(3a*S*,4*S*,6a*R*)-2-oxohexahydro-1*H*-thieno[3,4-*d*]imidazol-4-yl]pentanamide (15)

To the solution of **14** (116.0 mg, 0.26 mmol) in MeOH (2.0 mL) was added 10% Pd-C (wetted with ca. 55% water, 160.0 mg). After being stirred at rt overnight under H_2 atmosphere, the mixture was filtered through a celite pad and concentrated. The crude product was used for the next step without further purification.

4.1.7. 4-(4-{6-[(4-Methoxybenzyl)imino]-2,3,4,6-tetrahydrobenzo[*e*]pyrimido[1,2-*c*][1,3]thiazin-9-yl}benzoyl)benzyl {13-oxo-17-[(3a*S*,4*S*,6a*R*)-2-oxohexahydro-1*H*-thieno[3,4-*d*]imidazol-4-yl]-3,6,9-trioxa-12-azaheptadecyl}carbamate (17)

To a solution of **13** (157.2 mg, 0.20 mmol) in THF (2.0 mL) was added TBAF in THF (1 M, 0.50 mL, 0.50 mmol). After being stirred at rt overnight, the reaction mixture was quenched with satd NH_4Cl. The whole was extracted with $CHCl_3$ and dried over $MgSO_4$. After concentration, the residue was subjected to flash column chromatography over aluminum oxide with *n*-hexane/EtOAc (5:1–0:1) to give the desilylated compound. To a solution of the resulting compound in CH_2Cl_2 (6.0 mL) were added *p*-nitrophenyl chloroformate (60.5 mg, 0.30 mmol) and pyridine (64.6 μL, 0.8 mmol). After being stirred under reflux for 1 h, additional *p*-nitrophenyl chloroformate (12.0 mg, 0.06 mmol) was added. After being stirred under reflux for additional 30 min, the reaction mixture was washed with brine, and dried over $MgSO_4$. After concentration, the solution of resulting residue (crude **16**) in DMF (2.0 mL) was added to the solution of **15** (ca. 0.26 mmol) and Et_3N (86.7 μL) in DMF (3.0 mL). After being stirred at rt for 8 h, the reaction mixture was stirred at 40 °C overnight. After concentration, the residue was purified by flash column chromatography over aluminum oxide with $CHCl_3$/MeOH (1:0–95:5) followed by flash column chromatography over silica gel with $CHCl_3$/MeOH (1:0–9:1) to give the title compound **17** as pale yellow amorphous (90.6 mg, 46%): IR (neat) cm^{-1}: 1699 (C=O), 1656 (C=O), 1607 (C=N), 1511 (C=N); ^{1}H NMR (500 MHz, $CDCl_3$) δ: 1.39–1.45 (m, 2H, CH_2), 1.57–1.74 (m, 4H, 2 × CH_2), 2.03–2.08 (m, 2H, CH_2), 2.20 (t, J = 6.9 Hz, 2H, CH_2), 2.70 (d, J = 12.6 Hz, 1H, CH), 2.87 (dd, J = 12.6, 4.6 Hz, 1H, CH), 3.12 (d, J = 11.7, 4.6 Hz, 1H, CH), 3.40–3.43 (m, 4H, 2 × CH_2), 3.54–3.71 (m, 14H, 7 × CH_2), 3.77 (s, 3H, CH_3), 3.88 (t, J = 6.0 Hz, 2H, CH_2), 4.19 (s, 2H, CH_2), 4.26–4.29 (m, 1H, CH), 4.45–4.47 (m, 1H, CH), 5.17 (s, 1H, NH), 5.20 (s, 2H, CH_2), 5.65 (s, 1H, NH), 6.07 (s, 1H, NH), 6.48 (s, 1H, NH), 6.84 (d, J = 8.0 Hz, 2H, Ar), 7.26–7.28 (m, 2H, Ar), 7.44–7.62 (m, 7H, Ar), 7.81 (d, J = 8.0 Hz, 2H, Ar), 7.85 (d, J = 8.0 Hz, 2H, Ar); ^{13}C NMR (125 MHz, $CDCl_3$) δ: 19.8, 25.5, 28.0, 28.1, 35.9, 39.0, 39.1, 40.4, 40.9, 44.3, 47.7, 55.2, 55.5, 60.1, 61.7, 65.8, 69.9, 69.9, 70.0, 70.2, 70.3 (2C), 112.2, 114.0 (2C), 125.7, 127.1 (2C), 127.4 (2C), 127.6, 128.6, 129.5, 130.2 (2C), 130.3 (2C), 130.6 (2C), 135.0, 136.5, 136.7, 137.1, 141.4, 142.0, 143.7, 148.2, 156.3, 158.9, 163.9, 173.2, 195.7; HRMS (FAB): m/z calcd for $C_{52}H_{62}N_7O_9S_2$ $[M+H]^+$ 992.4050; found: 992.4050.

4.1.8. 4-[4-(6-Imino-2,3,4,6-tetrahydrobenzo[*e*]pyrimido[1,2-*c*][1,3]thiazin-9-yl)benzoyl]benzyl {13-oxo-17-[(3a*S*,4*S*,6a*R*)-2-oxohexahydro-1*H*-thieno[3,4-*d*]imidazol-4-yl]-3,6,9-trioxa-12-azaheptadecyl}carbamate (6)

TFA (2.0 mL) was added to a mixture of **17** (62.9 mg, 0.063 mmol) in small amount of $CHCl_3$ (1 or 2 drops) and molecular sieves 4 Å (300 mg, powder, activated by heating). After being stirred at rt for 4 h, Et_3N was added dropwise to the stirring mixture at 0 °C to adjust pH to 8–9. The whole was extracted with $CHCl_3$, and washed with satd $NaHCO_3$, brine, and dried over $MgSO_4$. After concentration, the residue was purified by flash chromatography over aluminum oxide with $CHCl_3$/MeOH (1:0–95:5) followed by preparative HPLC to give the title compound **6** as colorless solid (19.3 mg, 35%): IR (neat) cm^{-1}: 1699 (C=O), 1654 (C=O), 1621 (C=O), 1601 (C=N), 1574 (C=N); ^{1}H NMR (500 MHz, $CDCl_3$) δ: 1.39–1.44 (m, 2H, CH_2), 1.60–1.76 (m, 4H, 2 × CH_2), 1.99–2.04 (m, 2H, CH_2), 2.20 (t, J = 7.4 Hz, 2H, CH_2), 2.71 (d, J = 12.6 Hz, 1H, CH), 2.88 (dd, J = 12.6, 5.0 Hz, 1H, CH), 3.11 (d, J = 11.7, 5.0 Hz, 1H, CH), 3.40–3.43 (m, 4H, 2 × CH_2), 3.54–3.63 (m, 12H, 6 × CH_2), 3.73 (t, J = 5.4 Hz, 2H, CH_2), 4.06 (t, J = 6.0 Hz, 2H, CH_2), 4.28 (t, J = 6.0 Hz, 1H, CH), 4.47 (t, J = 6.0 Hz, 1H, CH), 5.20 (s, 2H, CH_2), 5.44 (s, 1H, NH), 5.73 (s, 1H, NH), 6.37 (s, 1H, NH), 6.66 (s, 1H, NH), 7.32 (s, 1H, Ar), 7.48 (d, J = 8.0 Hz, 2H, Ar), 7.52 (d, J = 8.6 Hz, 1H, Ar), 7.69 (d, J = 8.0 Hz, 2H, Ar), 7.81 (d, J = 8.0 Hz, 2H, Ar), 7.88 (d, J = 8.0 Hz, 2H, Ar), 8.36 (d, J = 8.6 Hz, 1H, Ar); ^{13}C NMR (125 MHz, $CDCl_3$) δ: 20.8, 25.6, 28.0, 28.2, 35.9, 39.0, 40.4, 40.9, 43.9, 44.7, 51.2, 55.6, 60.1, 61.7, 65.7, 69.9, 70.0, 70.1, 70.3 (2C), 122.0, 125.2, 125.8, 126.9 (2C), 127.4 (2C), 129.6, 129.7, 130.2 (2C), 130.7 (2C), 137.0, 141.5, 142.2, 142.9, 144.8, 146.6, 152.9, 156.3, 164.1, 173.3, 195.6; HRMS (FAB): m/z calcd for $C_{44}H_{54}N_7O_8S_2$ $[M+H]^+$ 872.3475; found: 872.3481.

4.1.9. *N*-[9-Bromo-1′-(4-methoxybenzyl)-2*H*-spiro(benzo[*e*]-pyrimido[1,2-*c*][1,3]thiazine-3,4′-piperidin)-6(4*H*)-ylidene]-1-(4-methoxyphenyl)methanamine (19)

By a procedure identical with that described for synthesis of **12** from **2a**, the imine **18** (274.3 mg, 0.57 mmol) was converted into **19** as colorless amorphous (275.1 mg, 81%): IR (neat) cm^{-1}: 1668 (C=N), 1510 (C=N); ^{1}H NMR (400 MHz, $CDCl_3$) δ: 1.61–1.64 (m, 4H, 2 × CH_2), 2.36–2.42 (m, 2H, CH_2), 2.45–2.51 (m, 2H, CH_2), 3.45 (s, 2H, CH_2), 3.47 (s, 2H, CH_2), 3.55 (s, 2H, CH_2), 3.80 (s, 3H, CH_3), 3.81 (s, 3H, CH_3), 4.12 (s, 2H, CH_2), 6.82-6.87 (m, 4H, Ar), 7.19–7.23 (m, 5H, Ar), 7.38 (dd, J = 8.2, 1.8 Hz, 1H, Ar), 7.44 (d, J = 2.0 Hz, 1H, Ar); ^{13}C NMR (100 MHz, $CDCl_3$) δ: 28.2, 32.4 (2C), 39.1, 48.7 (2C), 54.6, 55.2, 55.3, 55.4, 62.6, 111.9, 113.7 (2C), 113.9, 114.1 (2C), 124.8, 128.0, 129.7, 130.0, 130.2 (4C), 133.4, 133.4, 138.6, 147.1, 158.8, 159.1; HRMS (FAB): m/z calcd for $C_{31}H_{34}BrN_4O_2S$ $[M+H]^+$ 605.1586; found: 605.1585.

4.1.10. *N*-[9-Bromo-2*H*-spiro(benzo[*e*]pyrimido[1,2-*c*][1,3]-thiazine-3,4'-piperidin)-6(4*H*)-ylidene]-1-(4-methoxyphenyl)-methanamine (20)

To a solution of **19** (60.6 mg, 0.10 mmol) in CH_2Cl_2 (0.5 mL) were added Et_3N (28.9 μL, 0.20 mmol) and 1-chloroethyl chloroformate (21.8 μL, 0.20 mmol) at 0 °C under an Ar atmosphere. After being stirred at the same temperature for 30 min, the reaction mixture was concentrated. The residue was dissolved in MeOH (2.0 mL). After being stirred under reflux for 10 min, the reaction mixture was concentrated. The residue was dissolved in $CHCl_3$, and was washed with satd $NaHCO_3$, brine, and dried over $MgSO_4$. After concentration, the crude product was used for the next step without further purification.

4.1.11. 4-[4-(*tert*-Butyldiphenylsilyloxymethyl)benzoyl]benzyl {13-oxo-17-[(3a*S*,4*S*,6a*R*)-2-oxohexahydro-1*H*-thieno[3,4-*d*]imidazol-4-yl]-3,6,9-trioxa-12-azaheptadecyl}carbamate (23)

To a solution of **21**[20] (240.3 mg, 0.50 mmol) in CH_2Cl_2 (15.0 mL) were added *p*-nitrophenyl chloroformate (151.2 mg, 0.75 mmol) and pyridine (161.4 μL, 2.00 mmol). After being stirred under reflux for 1 h, the reaction mixture was washed with brine, and dried over $MgSO_4$. After concentration, the solution of the resulting residue in DMF (7.5 mL) was added to a mixture of **15** (ca. 0.20 mmol) and Et_3N (216.8 μL) in DMF (5.0 mL). After being stirred at rt overnight, the mixture was concentrated. The residue was purified by flash column chromatography over silica gel with $CHCl_3$/MeOH (1:0–95:5) to give the title compound **23** as colorless amorphous (471.5 mg, quant.): IR (neat) cm^{-1}: 1700 (C=O), 1656 (C=O), 1609 (C=O); ^1H NMR (400 MHz, $CDCl_3$) δ: 1.12 (s, 9H, 3 × CH_3), 1.39–1.46 (m, 2H, CH_2), 1.61–1.76 (m, 4H, 2 × CH_2), 2.19–2.23 (m, 2H, CH_2), 2.69–2.76 (m, 1H, CH), 2.85–2.90 (m, 1H, CH), 3.09–3.15 (m, 1H, CH), 3.39–3.43 (m, 4H, 2 × CH_2), 3.54–3.66 (m, 12H, 6 × CH_2), 4.26–4.33 (m, 1H, CH), 4.45–4.51 (m, 1H, CH), 4.85 (s, 2H, CH_2), 5.19 (s, 2H, CH_2), 5.54 (br s, 1H, NH), 5.68 (br s, 1H, NH), 6.55 (br s, 1H, NH), 6.72 (br s, 1H, NH), 7.36–7.48 (m, 10H, Ar), 7.69 (d, J = 7.6 Hz, 2H, Ar), 7.70 (d, J = 7.6 Hz, 2H, Ar), 7.77 (d, J = 5.5 Hz, 2H, Ar), 7.79 (d, J = 5.5 Hz, 2H, Ar); ^{13}C NMR (100 MHz, $CDCl_3$) δ: 19.3, 25.5, 26.8 (3C), 28.1, 28.2, 35.9, 39.1, 40.5, 40.9, 55.5, 60.1, 61.7, 65.1, 65.8, 69.9, 70.0, 70.0, 70.2, 70.4 (2C), 125.6 (2C), 127.4 (2C), 127.8 (4C), 129.8 (2C), 130.1 (2C), 130.2 (2C), 133.2 (2C), 135.5 (4C), 136.1, 137.4, 141.2, 146.0, 156.3 163.9, 173.2, 196.0; HRMS (FAB): m/z calcd for $C_{50}H_{65}N_4O_9SSi$ $[M+H]^+$ 925.4242; found: 925.4246.

4.1.12. 4-[4-(Hydroxymethyl)benzoyl]benzyl {13-oxo-17-[(3a*S*,4*S*,6a*R*)-2-oxohexahydro-1*H*-thieno[3,4-*d*]imidazol-4-yl]-3,6,9-trioxa-12-azaheptadecyl}carbamate (24)

To a solution of **23** (383.0 mg, 0.41 mmol) in THF (8.2 mL) was added HF-pyridine (617.7 μL) at 0 °C. After being stirred at rt overnight, the reaction was quenched with satd $NaHCO_3$. The whole was extracted with $CHCl_3$, and washed with water and brine, and dried over $MgSO_4$. After concentration, the residue was purified by preparative TLC over silica gel with $CHCl_3$/MeOH (85:15) to give the title compound **24** as colorless oil (204.2 mg, 73%): IR (neat) cm^{-1}: 1696 (C=O), 1650 (C=O), 1609 (C=O); ^1H NMR (400 MHz, $CDCl_3$) δ: 1.34–1.41 (m, 2H, CH_2), 1.55–1.73 (m, 4H, 2 × CH_2), 2.07 (br s, 1H, OH), 2.16 (t, J = 7.4 Hz, 2H, CH_2), 2.68 (d, J = 12.9 Hz, 1H, CH), 2.85 (dd, J = 12.9, 4.9 Hz, 1H, CH), 3.08 (dd, J = 11.8, 7.4 Hz 1H, CH), 3.37–3.42 (m, 4H, 2 × CH_2), 3.51–3.64 (m, 12H, 6 × CH_2), 4.23 (t, J = 6.2 Hz, 1H, CH), 4.43 (t, J = 6.2 Hz, 1H, CH), 4.78 (s, 2H, CH_2), 5.18 (s, 2H, CH_2), 5.51 (br s, 1H, NH), 5.82 (br s, 1H, NH), 6.34 (br s, 1H, NH), 6.75 (br s, 1H, NH), 7.45 (d, J = 8.3 Hz, 2H, Ar), 7.48 (d, J = 8.3 Hz, 2H, Ar), 7.76 (d, J = 8.0 Hz, 2H, Ar), 7.77 (d, J = 8.0 Hz, 2H, Ar); ^{13}C NMR (125 MHz, $CDCl_3$) δ: 25.5, 28.0, 28.2, 35.8, 39.1, 40.4, 40.9, 55.6, 60.2, 61.8, 64.2, 65.7, 69.9, 69.9 (2C), 70.1, 70.3 (2C), 126.4 (2C), 127.3 (2C), 130.2 (2C), 130.2 (2C), 136.2, 137.1, 141.3, 146.4, 156.4, 164.1, 173.5, 196.0; HRMS (FAB): m/z calcd for $C_{34}H_{47}N_4O_9S$ $[M+H]^+$ 687.3064; found: 687.3058.

4.1.13. 4-(4-{[(4-Nitrophenoxy)carbonyloxy]methyl}benzoyl)-benzyl 13-oxo-17-[(3a*S*,4*S*,6a*R*)-2-oxohexahydro-1*H*-thieno[3,4-*d*]imidazol-4-yl]-3,6,9-trioxa-12-azaheptadecylcarbamate (25)

To a solution of **24** (28.2 mg, 0.04 mmol) in CH_2Cl_2 (1.2 mL) were added *p*-nitrophenyl chloroformate (24.8 mg, 0.12 mmol) and pyridine (13.2 μL, 0.16 mmol). After being stirred under reflux for 1 h, the reaction mixture was washed with brine, and dried over $MgSO_4$. After concentration, the residue was purified by preparative TLC over aluminum oxide with $CHCl_3$/MeOH (9:1) to give the title compound **25** as colorless amorphous (27.9 mg, 80%): IR (neat) cm^{-1}: 1768 (C=O), 1698 (C=O), 1656 (C=O), 1612 (C=O); ^1H NMR (400 MHz, $CDCl_3$) δ: 1.38–1.45 (m, 2H, CH_2), 1.59–1.76 (m, 4H, 2 × CH_2), 2.20 (t, J = 7.4 Hz, 2H, CH_2), 2.72 (d, J = 12.7 Hz, 1H, CH), 2.88 (dd, J = 12.7, 4.9 Hz, 1H, CH), 3.12 (dd, J = 11.8, 7.4 Hz, 1H, CH), 3.38–3.44 (m, 4H, 2 × CH_2), 3.55–3.63 (m, 12H, 6 × CH_2), 4.28 (t, J = 6.0 Hz, 1H, CH), 4.47 (t, J = 6.0 Hz, 1H, CH), 5.19 (s, 2H, CH_2), 5.38 (s, 2H, CH_2), 5.52 (br s, 1H, NH), 5.69 (br s, 1H, NH), 6.44 (br s, 1H, NH), 6.66 (br s, 1H, NH), 7.41 (d, J = 9.3 Hz, 2H, Ar), 7.47 (d, J = 8.0 Hz, 2H, Ar), 7.56 (d, J = 8.0 Hz, 2H, Ar), 7.79 (d, J = 8.0 Hz, 2H, Ar), 7.84 (d, J = 8.0 Hz, 2H, Ar), 8.29 (d, J = 9.3 Hz, 2H, Ar); ^{13}C NMR ($CDCl_3$, 100 MHz) δ: 25.5, 28.1, 28.2, 35.9, 39.1, 40.5, 40.9, 55.5, 60.2, 61.8, 65.8, 69.9, 70.0, 70.0 (2C), 70.2, 70.4 (2C), 121.7 (2C), 125.3 (2C), 127.5 (2C), 128.1 (2C), 130.2 (2C), 130.4 (2C), 136.8, 137.9, 138.6, 141.7, 145.5, 152.4, 155.4, 156.3, 163.9, 173.3, 195.5; HRMS (FAB): m/z calcd for $C_{41}H_{50}N_5O_{13}S$ $[M+H]^+$ 852.3126; found: 852.3127.

4.1.14. 4-(4-{3,17-Dioxo-21-[(3a*S*,4*S*,6a*R*)-2-oxohexahydro-1*H*-thieno[3,4-*d*]imidazol-4-yl]-2,7,10,13-tetraoxa-4,16-diazahenicosyl}benzoyl)benzyl 9-bromo-6-imino-4,6-dihydro-2*H*-spiro(benzo[*e*]pyrimido[1,2-*c*][1,3]thiazine-3,4'-piperidine)-1'-carboxylate (7)

To a solution of **20** (ca. 0.027 mmol) in DMF (0.4 mL) were added Et_3N (11.7 μL, 0.081 mmol) and the solution of **25** (23.3 mg, 0.027 mmol) in DMF (0.4 mL) at rt. After being stirred at the same temperature for 1 h, the reaction mixture was concentrated. The residue was subjected to preparative TLC over silica gel with $CHCl_3$/MeOH (9:1) to give crude imine **26**. By a procedure identical with that described for synthesis of **6** from **17**, the crude **26** was converted into **7** as a colorless amorphous (10.4 mg, 36%): IR (neat) cm^{-1}: 1699 (C=O), 1655 (C=O), 1612 (C=O), 1573 (C=N); ^1H NMR (400 MHz, $CDCl_3$) δ: 1.39–1.46 (m, 2H, CH_2), 1.53 (d, J = 5.6 Hz, 4H, 2 × CH_2), 1.61–1.72 (m, 4H, 2 × CH_2), 2.20 (t, J = 7.3 Hz, 2H, CH_2), 2.71 (d, J = 12.7 Hz, 1H, CH), 2.89 (dd, J = 12.7, 4.9 Hz, 1H, CH), 3.12 (d, J = 12.1, 7.3 Hz, 1H, CH), 3.39–3.44 (m, 4H, 2 × CH_2), 3.53–3.63 (m, 18H, 9 × CH_2), 3.93 (s, 2H, CH_2), 4.28 (t, J = 5.7 Hz, 1H, CH), 4.47 (t, J = 6.5 Hz, 1H, CH), 5.14 (s, 1H, NH), 5.19 (s, 2H, CH_2), 5.22 (s, 2H, CH_2), 5.68 (s, 1H, NH), 6.01 (s, 1H, NH), 6.52 (s, 1H, NH), 7.22 (d, J = 2.0 Hz, 1H, Ar), 7.34 (dd, J = 8.8, 2.0 Hz, 1H, Ar), 7.45 (d, J = 8.0 Hz, 2H, Ar), 7.46 (d, J = 8.0 Hz, 2H, Ar), 7.79 (m, 4H, Ar), 8.10 (d, J = 8.8 Hz, 1H, Ar); ^{13}C NMR (100 MHz, $CDCl_3$) δ: 25.5, 28.1, 28.1, 29.6, 32.2 (2C), 35.8, 39.1, 39.9 (2C), 40.5, 40.9, 49.9, 54.6, 55.4, 60.1, 61.8, 65.8, 66.4, 69.9, 70.0 (2C), 70.2, 70.4 (2C), 125.0, 125.3, 126.0, 127.3 (2C), 127.4 (2C), 129.6, 130.2 (2C), 130.3 (2C), 130.4, 130.6, 137.0, 137.1, 141.4, 141.5, 145.1, 152.6, 155.0, 156.3, 163.8, 173.3, 195.7; HRMS (FAB): m/z calcd for $C_{50}H_{62}BrN_8O_{10}S_2$ $[M+H]^+$ 1077.3214; found: 1077.3213.

4.1.15. *N*-(*tert*-Butyl)-9-{4-[4-(*tert*-butyldiphenylsilyloxy)-methyl]benzoylphenyl}-3,4-dihydro-2*H*,6*H*-pyrimido[1,2-*c*][1,3]benzothiazin-6-imine (28)

Compound **27** (2.17 g, 6.17 mmol) was subjected to the general cross-coupling procedure as described for the synthesis of **13** to give the title compound **28** as colorless solid (3.16 g, 71%): mp 152–153 °C (from $CHCl_3$/*n*-hexane): IR (neat) cm^{-1}: 1656 (C=O), 1623 (C=N), 1593 (C=N); ^1H NMR (400 MHz, $CDCl_3$) δ: 1.12 (s, 9H, 3 × CH_3), 1.41 (s, 9H, 3 × CH_3), 1.91-1.97 (m, 2H), 3.65 (t, J = 5.4 Hz, 2H, CH_2), 3.90 (t, J = 6.2 Hz, 2H, CH_2), 4.86 (s, 2H, CH_2), 7.37-7.48 (m, 10H, Ar), 7.69-7.71 (m, 6H, Ar), 7.81 (d, J = 8.3 Hz, 2H, Ar), 7.88 (d, J = 8.3 Hz, 2H, Ar), 8.30 (d, J = 8.5 Hz, 1H, Ar); ^{13}C NMR (100 MHz, $CDCl_3$) δ: 19.3, 21.9, 26.8 (3C), 30.0 (3C), 45.2, 45.5, 54.2, 65.2, 123.0, 124.9, 125.7 (2C), 126.9 (2C), 127.4, 127.8 (4C), 129.1, 129.8 (2C), 129.9, 130.2 (2C), 130.7 (2C), 133.2 (2C), 135.5 (4C), 136.2, 137.2, 138.0, 141.7, 143.2, 146.1, 147.6, 195.9; HRMS (FAB): m/z calcd for $C_{45}H_{48}N_3O_2SSi$ $[M+H]^+$ 722.3237; found: 722.3244.

4.1.16. *N*-(*tert*-Butyl)-3,4-dihydro-9-[4-(4-propargyloxymethyl)-benzoylphenyl]-2*H*,6*H*-pyrimido[1,2-*c*][1,3]benzothiazin-6-imine (29)

To a solution of **28** (200.0 mg, 0.28 mmol) in THF (2.8 mL) was added TBAF in THF (1 M, 0.55 mL, 0.55 mmol). After being stirred at rt for 2 h, the reaction mixture was quenched with satd NH_4Cl. The whole was extracted with EtOAc, and washed with brine, and dried over $MgSO_4$. The filtrate was concentrated. To the solution of the resulting residue in THF (2.8 mL) was added NaH (22.8 mg, 0.55 mmol, 60% oil suspension) at 0 °C. After being stirred at the same temperature for 30 min, propargyl bromide (31.5 μL, 0.42 mmol) was added dropwise. After being stirred at rt overnight, the reaction was quenched with water. The whole was extracted with EtOAc, and washed with brine, and dried over $MgSO_4$. After concentration, the residue was purified by flash column chromatography over aluminum oxide with *n*-hexane/EtOAc (5:1) to give the title compound **29** as colorless solid (87.2 mg, 60%): mp 133–135 °C (from $CHCl_3$/*n*-hexane): IR (neat) cm^{-1}: 1656 (C=O), 1620 (C=N), 1593 (C=N); ^1H NMR (400 MHz, $CDCl_3$) δ: 1.41 (s, 9H, 3 × CH_3), 1.91–1.97 (m, 2H), 2.50 (t, J = 2.3 Hz, 1H, CH), 3.65 (t, J = 5.5 Hz, 2H, CH_2), 3.90 (t, J = 6.1 Hz, 2H, CH_2), 4.25 (d, J = 2.3 Hz, 2H, CH_2), 4.71 (s, 2H, CH_2), 7.39 (d, J = 1.7 Hz, 1H, Ar), 7.46–7.50 (m, 3H, Ar), 7.70 (d, J = 8.0 Hz, 2H, Ar), 7.82 (d, J = 8.0 Hz, 2H, Ar), 7.87 (d, J = 8.0 Hz, 2H, Ar), 8.30 (d, J = 8.3 Hz, 1H, Ar); ^{13}C NMR (100 MHz, $CDCl_3$) δ: 21.9, 30.0 (3C), 45.2, 45.4, 54.2, 57.6, 70.9, 75.0, 79.3, 123.0, 124.8, 126.9 (2C), 127.3, 127.5 (2C), 129.1, 129.9, 130.2 (2C), 130.7 (2C), 136.9, 137.0, 137.9, 141.6, 142.2, 143.4, 147.5, 195.7; HRMS (FAB): m/z calcd for $C_{32}H_{32}N_3O_2S$ $[M+H]^+$ 522.2215; found: 522.2207.

4.1.17. 3,4-Dihydro-9-[4-(4-propargyloxymethyl)-benzoylphenyl]-2*H*,6*H*-pyrimido[1,2-*c*][1,3]benzothiazin-6-imine (8)

Using a procedure identical with that described for synthesis of **6** from **17**, the imine **29** (42.8 mg, 0.08 mmol) was allowed to react under reflux for 1 h with TFA (2.0 mL) and MS4Å (300 mg). Purification by flash chromatography over aluminum oxide with *n*-hexane/EtOAc (9:1 to 1:1) gave the title compound **8** as colorless solid (35.4 mg, 92%): mp 159–160 °C (from $CHCl_3$/*n*-hexane): IR (neat) cm^{-1}: 1654 (C=O), 1619 (C=N), 1573 (C=N); ^1H NMR (400 MHz, $CDCl_3$) δ: 1.96–2.04 (m, 2H), 2.50 (t, J = 2.4 Hz, 1H, CH), 3.72 (t, J = 5.6 Hz, 2H, CH_2), 4.05 (t, J = 6.1 Hz, 2H, CH_2), 4.25 (d, J = 2.4 Hz, 2H, CH_2), 4.71 (s, 2H, CH_2), 7.26–7.31 (m, 2H, Ar, NH), 7.48–7.51 (m, 3H, Ar), 7.67–7.89 (m, 6H, Ar), 8.33 (d, J = 8.5 Hz, 1H, Ar); ^{13}C NMR (100 MHz, $CDCl_3$) δ: 21.0, 43.8, 45.0, 57.6, 70.9, 75.0, 79.3, 122.0, 125.1, 126.3, 126.9 (2C), 127.5 (2C), 129.6, 129.7, 130.2 (2C), 130.7 (2C), 137.0, 137.1, 142.2, 142.3, 143.0, 146.2, 153.0, 195.7; HRMS (FAB): m/z calcd for $C_{28}H_{24}N_3O_2S$ $[M+H]^+$ 466.1589; found: 466.1589.

4.2. Determination of anti-HIV activity

The sensitivity of HIV-1_{IIIB} strain was determined by the MAGI assay. The target cells (HeLa-CD4/CCR5-LTR/β-gal; 10^4 cells/well) were plated in 96-well flat microtiter culture plates. On the following day, the cells were inoculated with the HIV-1 (60 MAGI U/well, giving 60 blue cells after 48 h of incubation) and cultured in the presence of various concentrations of the test compounds in fresh medium. Forty-eight hours after viral exposure, all the blue cells stained with X-Gal (5-bromo-4-chloro-3-indolyl-β-D-galactopyranoside) were counted in each well. The activity of test compounds was determined as the concentration that blocked HIV-1 infection by 50% (50% effective concentration [EC_{50}]). EC_{50} was determined by using the following formula:

$$EC_{50} = 10^{\wedge}[\log(A/B) \times (50 - C)/(D - C) + \log(B)]$$

wherein

A: of the two points on the graph which bracket 50% inhibition, the higher concentration of the test compound,

B: of the two points on the graph which bracket 50% inhibition, the lower concentration of the test compound,

C: inhibitory activity (%) at the concentration B,

D: inhibitory activity (%) at the concentration A.

4.3. Photoaffinity labeling experiments using HIV-1-infected H9 cells (H9IIIB)

1 μL of probe **6** or **7** (10 mM solution in DMSO) was added to H9 cells chronically infected with HIV-1 (H9IIIB) in D-MEM with 10% fetal bovine serum (500 μL, 0.5 × 10^6 cells). For the competitive evaluation (Fig. 3, lane C), 2 μL of compound **3a** (10 mM solution in DMSO) was also added. The cells were incubated at 37 °C for 1 h. Then the cells were photolabeled by irradiation by UV (MUV-202U, Moritex Co., Japan) at room temperature for 1 min at a distance of 3 cm through a longpass filter (LU0300, Asahi spectra Co.). The mixture was centrifuged at 200 × g for 5 min and the supernatant was removed. The cells were washed with PBS once and were lysed in RIPA buffer containing 1% protease inhibitor cocktail (Nacalai Tesque, Inc., Japan) at 4 °C for 30 min. After centrifugation at 16500 × g for 15 min, the supernatant was used for the next experiment.

NeutrAvidin-agarose beads (50 μL, Thermo), which were equilibrated with RIPA buffer, were treated with the supernatant containing 180 μg of proteins and were incubated at 4 °C for 1 h. The beads were then centrifuged at 9100 × g for 30 sec and washed with RIPA buffer (repeated three times). After heating the beads at 95 °C for 5 min in sample buffer [50 mM Tris–HCl (pH 8.0), 2% SDS, 0.1% BPB, 10% glycerol, 2% β-ME], the supernatants were subjected to SDS–PAGE electrophoresis (SuperSep™Ace, 5–20%, Wako) and the separated proteins were transferred onto a PVDF membrane. The membrane was blocked with Blocking One (Nacalai Tesque, Inc.) at room temperature for 1 h, and was then incubated with a streptavidin–HRP conjugate (Invitrogen; 1:5000 in PBS with 0.1% Tween) at 4 °C overnight. The membrane was treated with Chemi-Lumi One L (Nacalai Tesque, Inc.). Biotinylated proteins were detected by Image Quant LAS 4000mini (GE Healthcare).

Acknowledgments

This work was supported by Grants-in-Aid for Scientific Research and Platform for Drug Discovery, Informatics, and Structural Life Science from MEXT; and Health and Labor Science Research

Grants (Research on HIV/AIDS, Japan). T.M. is grateful for JSPS Research Fellowships for Young Scientists.

Supplementary data

Supplementary data associated with this article can be found, in the online version, at http://dx.doi.org/10.1016/j.bmc.2013.01.016.

References and notes

1. PD 404182 (**1**) was previously reported to exhibit antimicrobial activity by inhibition of 3-deoxy-D-manno-octulosonic acid 8-phosphate synthase[2] or phosphopantetheinyl transferase.[3]
2. Birck, M. R.; Holler, T. P.; Woodard, R. W. *J. Am. Chem. Soc.* **2000**, *122*, 9334.
3. (a) Duckworth, B. P.; Aldrich, C. C. *Anal. Biochem.* **2010**, *403*, 13; (b) Foley, T. L.; Yasgar, A.; Garcia, C. J.; Jadhav, A.; Simeonov, A.; Burkart, M. D. *Org. Biomol. Chem.* **2010**, *8*, 4601.
4. Chockalingam, K.; Simeon, R. L.; Rice, C. M.; Chen, Z. *Proc. Natl. Acad. Sci. U.S.A.* **2010**, *107*, 3764.
5. Mizuhara, T.; Oishi, S.; Ohno, H.; Shimura, K.; Matsuoka, M.; Fujii, N. *Org. Biomol. Chem.* **2012**, *10*, 6792.
6. Mizuhara, T.; Oishi, S.; Ohno, H.; Shimura, K.; Matsuoka, M.; Fujii, N. *Bioorg. Med. Chem.* **2012**, *20*, 6434.
7. Mizuhara, T.; Inuki, S.; Oishi, S.; Fujii, N.; Ohno, H. *Chem. Commun.* **2009**, 3413.
8. Mizuhara, T.; Oishi, S.; Fujii, N.; Ohno, H. *J. Org. Chem.* **2010**, *75*, 265.
9. Baba, M.; Scgols, D.; Pauwels, R.; Nakashima, H.; De Clercq, E. *J. Acquir. Immune Defic. Syndr.* **1990**, *3*, 493.
10. (a) Kilby, J. M.; Eron, J. J. *N. Engl. J. Med.* **2003**, *348*, 2228; (b) Lalezari, J. P.; Henry, K.; O'Hearn, M.; Montaner, J. S.; Piliero, P. J.; Trottier, B.; Walmsley, S.; Cohen, C.; Kuritzkes, D. R.; Eron, J. J., Jr.; Chung, J.; DeMasi, R.; Donatacci, L.; Drobnes, C.; Delehanty, J.; Salgo, M. *N. Engl. J. Med.* **2003**, *348*, 2175; (c) Matthews, T.; Salgo, M.; Greenberg, M.; Chung, J.; DeMasi, R.; Bolognesi, D. *Nat. Rev. Drug Discov.* **2004**, *3*, 215.
11. (a) Dorr, P.; Westby, M.; Dobbs, S.; Griffin, P.; Irvine, B.; Macartney, M.; Mori, J.; Rickett, G.; Smith-Burchnell, C.; Napier, C.; Webster, R.; Armour, D.; Price, D.; Stammen, B.; Wood, A.; Perros, M. *Antimicrob. Agents Chemother.* **2005**, *49*, 4721; (b) Fätkenheuer, G.; Pozniak, A. L.; Johnson, M. A.; Plettenberg, A.; Staszewski, S.; Hoepelman, A. I. M.; Saag, M. S.; Goebel, F. D.; Rockstroh, J. K.; Dezube, B. J.; Jenkins, T. M.; Medhurst, C.; Sullivan, J. F.; Ridgway, C.; Abel, S.; James, I. T.; Youle, M.; Van Der Ryst, E. *Nat. Med.* **2005**, *11*, 1170; (c) Skerlj, R.; Bridger, G.; Zhou, Y.; Bourque, E.; McEachern, E.; Langille, J.; Harwig, C.; Veale, D.; Yang, W.; Li, T.; Zhu, Y.; Bey, M.; Baird, I.; Satori, M.; Metz, M.; Mosi, R.; Nelson, K.; Bodart, V.; Wong, R.; Fricker, S.; Huskens, D.; Schols, D. *Bioorg. Med. Chem. Lett.* **2011**, *21*, 6950.
12. (a) Bridger, G. J.; Skerlj, R. T.; Thornton, D.; Padmanabhan, S.; Martellucci, S. A.; Henson, G. W.; Abrams, M. J.; Yamamoto, N.; De Vreese, K.; Pauwels, R.; De Clercq, E. *J. Med. Chem.* **1995**, *38*, 366; (b) Bridger, G. J.; Skerlj, R. T.; Hernandez-Abad, P. E.; Bogucki, D. E.; Wang, Z.; Zhou, Y.; Nan, S.; Boehringer, E. M.; Wilson, T.; Crawford, J.; Metz, M.; Hatse, S.; Princen, K.; De Clercq, E.; Schols, D. *J. Med. Chem.* **2010**, *53*, 1250; (c) Fujii, N.; Oishi, S.; Hiramatsu, K.; Araki, T.; Ueda, S.; Tamamura, H.; Otaka, A.; Kusano, S.; Terakubo, S.; Nakashima, H.; Broach, J. A.; Trent, J. O.; Wang, Z.-X.; Peiper, S. C. *Angew. Chem., Int. Ed.* **2003**, *42*, 3251; (d) Ueda, S.; Oishi, S.; Wang, Z.-X.; Araki, T.; Tamamura, H.; Cluzeau, J.; Ohno, H.; Kusano, S.; Nakashima, H.; Trent, J. O.; Peiper, S. C.; Fujii, N. *J. Med. Chem.* **2007**, *50*, 192; (e) Inokuchi, E.; Oishi, S.; Kubo, T.; Ohno, H.; Shimura, K.; Matsuoka, M.; Fujii, N. *ACS Med. Chem. Lett.* **2011**, *2*, 477.
13. Chamoun, A. M.; Chockalingam, K.; Bobardt, M.; Simeon, R.; Chang, J.; Gallay, P.; Chen, Z. *Antimicrob. Agents Chemother.* **2012**, *56*, 672.
14. (a) Dorman, G.; Prestwich, G. D. *Biochemistry* **1994**, *33*, 5661; (b) Kotzyba-Hibert, F.; Kapfer, I.; Goeldner, M. *Angew. Chem., Int. Ed. Engl.* **1995**, *34*, 1296; (c) Fleming, S. A. *Tetrahedron* **1995**, *51*, 12479; (d) Tomohiro, T.; Hashimoto, M.; Hatanaka, Y. *Chem. Rec.* **2005**, *5*, 385.
15. (a) Drake, R. R.; Neamati, N.; Hong, H.; Pilon, A. A.; Sunthankar, P.; Hume, S. D.; Milne, G. W. A.; Pommier, Y. *Proc. Natl. Acad. Sci. U.S.A.* **1998**, *95*, 4170; (b) Lin, W.; Li, K.; Doughty, M. B. *Bioorg. Med. Chem.* **2002**, *10*, 4131; (c) Al-Mawsawi, L. Q.; Fikkert, V.; Dayam, R.; Witvrouw, M.; Burke, T. R., Jr.; Borchers, C. H.; Neamati, N. *Proc. Natl. Acad. Sci. U.S.A.* **2006**, *103*, 10080.
16. (a) Hofmann, K.; Kiso, Y. *Proc. Natl. Acad. Sci. U.S.A.* **1976**, *73*, 3516; (b) Hatanaka, Y.; Hashimoto, M.; Kanaoka, Y. *Bioorg. Med. Chem.* **1994**, *2*, 1367; (c) Kinoshita, T.; Cano-Delgado, A.; Seto, H.; Hiranuma, S.; Fujioka, S.; Yoshida, S.; Chory, J. *Nature* **2005**, *433*, 167; (d) Kotake, Y.; Sagane, K.; Owa, T.; Mimori-Kiyosue, Y.; Shimizu, H.; Uesugi, M.; Ishihama, Y.; Iwata, M.; Mizui, Y. *Nat. Chem. Biol.* **2007**, *3*, 570.
17. For examples of alkyne-conjugated photoaffinity probes with benzophenone see: (a) Ballell, L.; Alink, K. J.; Slijper, M.; Versluis, C.; Liskamp, R. M.; Pieters, R. J. *ChemBioChem* **2005**, *6*, 291; (b) Sieber, S. A.; Niessen, S.; Hoover, H. S.; Cravatt, B. F. *Nat. Chem. Biol.* **2006**, *2*, 274; (c) Salisbury, C. M.; Cravatt, B. F. *Proc. Natl. Acad. Sci. U.S.A.* **2007**, *104*, 1171; (d) Kalesh, K. A.; Sim, D. S.; Wang, J.; Liu, K.; Lin, Q.; Yao, S. Q. *Chem. Commun.* **2010**, *46*, 1118; (e) Eirich, J.; Orth, R.; Sieber, S. A. *J. Am. Chem. Soc.* **2011**, *133*, 12144.
18. Jiang, Q.; Ryan, M.; Zhichkin, P. *J. Org. Chem.* **2007**, *72*, 6618.
19. Fusz, S.; Srivatsan, S. G.; Ackermann, D.; Famulok, M. *J. Org. Chem.* **2008**, *73*, 5069.
20. Denholm, A. A.; George, M. H.; Hailes, H. C.; Tiffin, P. J.; Widdowson, D. A. *J. Chem. Soc., Perkin Trans. 1* **1995**, *5*, 541.
21. Watanabe, K.; Negi, S.; Sugiura, Y.; Kiriyama, A.; Honbo, A.; Iga, K.; Kodama, E. N.; Naitoh, T.; Matsuoka, M.; Kano, K. *Chem. Asian J.* **2010**, *5*, 825.

研究成果の刊行に関する一覧表

研究分担者　国立感染症研究所エイズ研究センター　村上　努

雑誌

発表者氏名	論文タイトル名	発表誌名	巻号	ページ	出版年
Aoki, T., S. Shimizu, E. Urano, Y. Futahashi, M, Hamatake, H. Tamamura, K. Terashima, T. Murakami, N. Yamamoto, and J. Komano.	Improvement of lentiviral vector-mdeaited gene transduction by genetic engineering of the structural protein Pr55Gag.	Gene Therapy	17	1124-1133	2010
Nakahara, T., W. Nomura, K. Ohba, A. Ohya, T. Tanaka, C. Hashimoto, T. Narumi, T. Murakami, N. Yamamoto and H. Tamamura.	Remodeling of Dynamic Structures of HIV-1 Envelope Proteins Leads to Synthetic Antigen Molecules Inducing Neutralizing Antibodies.	Bioconjugate Chem	21(4)	709-714	2010
Murakami, T and N. Yamamoto.	The role of CXCR4 in HIV infection and its potential as a therapeutic target (Review).	Future Microbiology	5(7)	1025-1039	2010
Tanaka T, Narumi T, Ozaki T, Sohma A, Ohashi N, Hashimoto C, Itotani K, Nomura W, Murakami T, Yamamoto N, Tamamura H.	Azamacrocyclic-metal complexes as CXCR4 antagonists.	Chem Med Chem	6	834-839	2011
Yanagita H, Urano E, Mastumoto K, Ichikawa R, Takaesu Y, Ogata M, Murakami T, Wu H, Chiba J, Komano J, Hosino T.	Structural and biochemical study on the inhibitory activity of derivatives of 5-nitro-furan-2-carboxylic acid for RNase H function of HIV-1 reverse transcriptase.	Bioorg Med Chem	19	816-825	2011
Narumi T, Aikawa H, Tanaka T, Hashimoto C, Ohashi N, Nomura W, Kobayakawa T, Takano H, Hirota Y, Murakami T, Yamamoto N, Tamamura H.	Low-molecular-weight CXCR4 ligands with variable spacers.	Chem Med Chem	8(1)	118-124	2012
Takemura T, Murakami T	Functional constraints on HIV-1 capsid: their impacts on the viral immune escape potency.	Front Microbiol	3	369	2012

Miyauchi K, Urano E, Takeda S, Murakami T, Okada Y, Cheng K, Yin H, Kubo M, Komano J	Toll-like receptor (TLR) 3 as a surrogate sensor of retroviral infection in human cells.	Biochem Biophys Res Commun	424 (3)	519-523	2012
Nakasone T, Kumakura S, Yamamoto M, Murakami T, Yamamoto N	Single oral administration of the novel CXCR4 antagonist, KRH-3955, induces an efficient and long-lasting increase of white blood cell count in normal macaques, and prevents CD4 depletion in SHIV-infected macaques.	Med Microbiol Immunol	202 (2)	175-182	2012
Nakasone T, Murakami T, Yamamoto N	Double oral administrations of emtricitabine/tenofovir prior to virus exposure protects against highly pathogenic SHIV infection in macaques.	Jpn J Infect Dis	65	345-349	2012
Narumi T, Tanaka T, Hashimoto C, Nomura W, Aikawa W, Sohma A, Itotani K, Kawamata M, Murakami T, Yamamoto N, Tamamura H	Pharmacophore-based small molecule CXCR4 ligands.	Biorg Med Chem Lett	22	4169-4172	2012
Yanagita H, Fudo S, Urano E, Ichikawa R, Ogata M, Yokota Y, Murakami T, Wu H, Chiba J, Komano J, Hoshino T:	Structural modulation study of inhibitory compounds for RNase H activity of HIV-1 reverse transcriptase.	Chem Pharm Bull	60	764-771	2012
竹村太地郎、村上　努	宿主とのインターフェイスとしてのHIV-1キャプシドタンパク質の役割	J AIDS Res	14(2)	10-15	2012
村上　努、高橋秀実	HIV と闘う宿主防御因子序論	J AIDS Res	14(1)	1-2	2012
Narumi T, Komoriya M, Hashimoto C, Wu H, Nomura W, Suzuki S, Tanaka T, Chiba J, Yamamoto N, Murakami T, Tamamura H.	Conjugation of cell-penetrating peptides leads to identification of anti-HIV peptides from matrix proteins.	Bioorg Med Chem	20	1468-1474	2012
M. A. Checkley, B. G. Luttge, P. Y. Mercredi, S. K. Kyere, J. Donlan, Murakami T, M. F. Summers, S. Cocklin, E. O. Freed	Reevaluation of the requirement for TIP47 in human immunodeficiency virus type 1 envelope glycoprotein incorporation.	J Virol	87(6)	3561-3570	2013

Takemura T, Kawamata M, Urabe M, Murakami T	Cyclophilin A-dependent restriction to capsid N121K mutant human immunodeficiency virus type 1 in a broad range of cell lines.	J Virol	87(7)	4086-4090	2013